ANKARA YILDIRIM BEYAZIT UNIVERSITY

GRADUATE SCHOOL OF NATURAL AND APPLIED SCIENCES

A GaN-BASED BI-DIRECTIONAL NON-INVERTING BUCK-BOOST CONVERTER

M.Sc. Thesis by

Hüseyin URAL

Department of Electrical and Electronics Engineering

July, 2024

ANKARA

A GaN-BASED BI-DIRECTIONAL NON-INVERTING BUCK-BOOST CONVERTER

A Thesis Submitted to

The Graduate School of Natural and Applied Sciences of

Ankara Yıldırım Beyazıt University

In Partial Fulfillment of the Requirements for the Degree of Master of Science in Electrical and Electronics Engineering, Department of Electrical and Electronics Engineering

by

Hüseyin URAL

July, 2024

ANKARA

M.Sc. THESIS EXAMINATION RESULT FORM

We have read the thesis entitled **"A GaN-BASED BI-DIRECTIONAL NON-INVERTING BUCK-BOOST CONVERTER"** completed by **HÜSEYİN URAL** under the supervision of **Prof. Dr. AHMET KARAARSLAN** and we certify that in our opinion it is fully adequate, in scope and in quality, as a thesis for the degree of Master of Science.

Prof. Dr. Ahmet KARAARSLAN

Supervisor

Prof. Dr. K. Çağatay BAYINDIR

Jury Member

Doç. Dr. Emre ÖZKOP

Jury Member

Prof. Dr. Sadettin ORHAN

Director

Graduate School of Natural and Applied Sciences

ETHICAL DECLARATION

I hereby declare that, in this thesis which has been prepared in accordance with the Thesis Writing Manual of Graduate School of Natural and Applied Sciences,

- All data, information and documents are obtained in the framework of academic and ethical rules,
- All information, documents and assessments are presented in accordance with scientific ethics and morals,
- All the materials that have been utilized are fully cited and referenced,
- No change has been made on the utilized materials,
- All the works presented are original,

and in any contrary case of above statements, I accept to renounce all my legal rights.

Date: 31.07.2024 **Signature: ……...**

Name & Surname:…….

ACKNOWLEDGMENTS

Firstly, I would like to express my sincere gratitude to my supervisor, Prof. Dr. Ahmet KARAARSLAN for his tremendous support and motivation during my study. His immense knowledge and precious recommendations constituted the milestones of this study. His guidance assisted me all the time of my research and while writing this thesis. I would also like to extend my deepest gratitude to Merve Nur URAL, played a decisive role in software design.

2024, 31 July **Hüseyin URAL**

A GaN-BASED BI-DIRECTIONAL NON-INVERTING BUCK-BOOST CONVERTER

ABSTRACT

In this study, a GaN-FET-based bidirectional non-inverting Buck-Boost converter has been designed using a PI control method to enhance efficiency, achieve significant reductions in circuit size, and create high power density. GaN-FETs are widely used due to their compact size and high energy transfer capacities. In power electronics, power density and efficiency are among the most critical technological factors in inverter modules. Advancements in switching technology have made GaN-FET-based semiconductor switching equipment more accessible, allowing for more efficient switching at higher frequencies. As a result, circuits can operate at higher power levels within smaller volumes.

The non-inverting Buck-Boost converter topology used in this thesis operates at a high switching frequency of 500 kHz, which is extremely challenging to achieve with conventional semiconductors. The circuit topology enables regulation over a wide input voltage range with minimal passive components. The symmetrical structure of the circuit allows it to operate in both directions (from input to output or from output to input), and by optimizing the controller, energy is transferred to the input side when the output voltage increases, thereby ensuring high performance. Efficient operation is achieved both in energy-consuming and energy-producing loads (such as regenerative braking). Features like high current and high voltage protection are adapted to the control topology to ensure safe operation across dynamic sources, dynamic loads, and wide input voltage ranges.

Keywords: GaN-FET, High Power Density, Buck-Boost Converter, PI Control

GaN-TABANLI ÇİFT YÖNLÜ EVİRMEYEN BUCK-BOOST DÖNÜŞTÜRÜCÜ

ÖZ

Bu çalışmada verimliliği artırmak, devre boyutunda önemli bir azalma sağlamak ve yüksek güç yoğunluğu oluşturmak için PI kontrol yöntemi kullanılarak GaN-FET tabanlı çift yönlü evirmeyen Buck-Boost dönüştürücü tasarlanmıştır.

GaN-FET'ler, az yer kaplayan yüksek enerji aktarım kapasitelerinden dolayı yaygın olarak kullanılmaktadır. Güç elektroniğinde, invertör modüllerinde güç yoğunluğu ve verimlilik en önemli teknoloji faktörleri arasında yer almaktadır. Anahtarlama teknolojisindeki gelişmeler sayesinde. GaN-FET tabanlı yarı iletken anahtarlama ekipmanları, bu teknolojideki gelişmelere bağlı olarak daha erişilebilir hale gelmektedir. Anahtarlama hem daha verimli hem de daha yüksek frekanslarda yapılabiliyor ve bunun sonucunda devreler daha küçük hacimde daha yüksek güçlerde çalışabiliyor.

Bu tezde kullanılan evirmeyen buck-boost dönüştürücü topolojisi, sıradan yarı iletkenlerle elde edilmesi son derece zor olan 500 kHz'lik yüksek bir anahtarlama frekansında çalışması sağlandı. Devre topolojisi sayesinde en az pasif elemanla en geniş giriş voltaj aralığını düzenleyebilmektedir. Devrenin simetrik yapısı her iki yönde de (girişten çıkışa veya çıkıştan girişe) çalışmasına olanak tanır ve kontrolcü optimize edilerek çıkış voltajının artması durumunda enerji giriş tarafına aktarılır, böylece yüksek performans sağlanır. Hem enerji tüketen hem de enerji üreten yüklerde (rejeneratif frenleme vb.) verimli çalışma sağlanır. Yüksek akım ve yüksek voltaj koruması gibi özellikler kontrol topolojisine uyarlanarak dinamik kaynak, dinamik yük ve geniş giriş voltajı aralıklarında güvenli çalışma sağlanır.

Anahtar Kelimeler: GaN-FET, Yüksek Güç Yoğunluğu, Buck-Boost Dönüştürücü, PI kontrol

CONTENTS

NOMENCLATURE

Roman Letter Symbols

A	: Current
D	: Duty Ratio
f	: Frequency
I	: Current
k	: Kilo
M	: Mega
m	: Mili
n	: Nano
T	: Period
u	: Micro
V	: Voltage

Greek Letter Symbols

Δ	: Difference
°	: Degree
ϕ	: Magnetic Flux
μ	: Magnetic Permeability
Ω	: Ohm

Subscripts

max	: Maximum
min	: Minimum

Acronyms

AC : Alternating Current

ADC : Analog to Digital Converter

AlGaN : Aluminium Gallium Nitride

ALN : Aluminium Nitride

CAGR : Compound Annual Growth Rate

DC : Direct Current

EMC : Electromagnetic Compability

EMI : Electromagnetic Interferance

EN : Enable

ESL : Equivalent Series Inductance

ESR : Equivalent Series Resistance

EV : Electric Vehicle

FET : Field Effect Transistor

GaN : Gallium Nitride

Hz : Hertz

IEEE : Institute of Electrical and Electronics Engineers

IRDS : International Roadmap for Devices and Systems

KCL : Kirchoff's Current Law

KVL : Kirchoff's Voltage Law

LDO : Low Dropout Regulator

Mbps : Mega Bit Per Second

MCU : Micro Controller Unit

MIPS : Million Instruction Per Second

MOCVD : Metal Oxide Chemical Vapor Deposition

MOSFET : Metal Oxide Field Effect Transistor

NTC : Negative Temperature Coefficient

OCC : One Cycle Control

OCV : Open Circuit Voltage

PCB : Printed Circuit Board

PI : Proportion-Integration

PID : Proportion-Integration-Derivation

PSMA : Power Sources Manufacturers Association

PWM : Pulse Width Modulation

RθJC : Thermal resistance to case

RC : Resistor-Capacitor

RDS : Drain-Source Resistance

SEPIC : Single Ended Primary Inductor Converter

SiC : Silicon Carbide

SMC : Sliding Mode Control

LIST OF TABLES

LIST OF FIGURES

CHAPTER 1

INTRODUCTION

In recent years, the quest for more efficient and compact power electronic systems has driven the development of advanced semiconductor materials and topologies for DC-DC converters. Among these innovations, Gallium Nitride (GaN) technology has emerged as a transformative force, revolutionizing the field of power electronics. GaN-FETs unique material properties, such as high electron mobility and breakdown voltage, make it an ideal candidate for high frequency and high-efficiency power conversion applications [1].

One of the notable applications of GaN-FETs technology is in the realm of DC-DC converters, particularly in non-inverting buck-boost converters. These converters play a pivotal role in a wide range of electronic devices and systems, offering voltage regulation and power conversion capabilities across a broad input voltage range [2-4]. The incorporation of GaN-FET devices into non-inverting buck-boost converters has opened new horizons for power electronics engineers, enabling the design of more efficient, compact, and versatile systems.

The importance of small-sized DC-DC converters in today's technological landscape cannot be overstated. These compact devices serve as the critical backbone for the miniaturization and portability of a vast array of electronic gadgets, from smartphones and laptops to wearable health monitors and IoT sensors [5]. Their ability to efficiently convert and regulate voltage levels within confined spaces empowers the design of sleek, lightweight, and energy-efficient devices [6-8].

The significance of the non-inverting buck-boost converter lies not only in its capability to efficiently convert input voltages within a broad range but also in its adaptability to handle dynamic input sources and varying output loads [9]. This adaptability makes it a preferred choice in applications where power sources may be intermittent, such as renewable energy systems, or where the load demands fluctuate,

as in battery management systems. Moreover, it plays a pivotal role in modern portable electronic devices, ensuring stable power delivery across varying battery voltages.

This paper describes the design and implementation of bidirectional GaN-FET Buck-Boost converter for high power density with Continues Conduction Mode (CCM) operated at 150W. In general, the paper is organized as follows: Chapter 2 clarifies the operation mode of the bi-directional converter in CCM and identify the converter parameters, discusses the proposed control method used for the converter. In Chapter 3 the operation of the Non-Inverting Bidirectional Buck-Boost converter is validated through simulation and experimental results, respectively. Chapter 4 summarizes the main findings in this study.

1.1 Technology of Switching Components

1.1.1 Gan Fets

Gallium nitride transistors bring tremendous performance and size advantages over silicon. These advantages can be applied to gain efficiency advantages, size advantages, or a combination of both, with application requirements and a coststructure that are similar to silicon [1]. GaN FETs in high-frequency, high-power applications due to their wide bandgap, which allows for faster switching speeds, higher thermal conductivity, and greater breakdown voltage. These characteristics enable GaN FETs to significantly reduce energy losses and enhance the efficiency of power conversion systems. Additionally, research from the Power Sources Manufacturers Association (PSMA) emphasizes that GaN FETs are critical for the development of compact, efficient power supplies and are increasingly being adopted in consumer electronics, data centers, and electric vehicles [10]. The ability of GaN FETs to operate at higher voltages and temperatures with greater efficiency positions them as key enablers of next generation electronic systems.

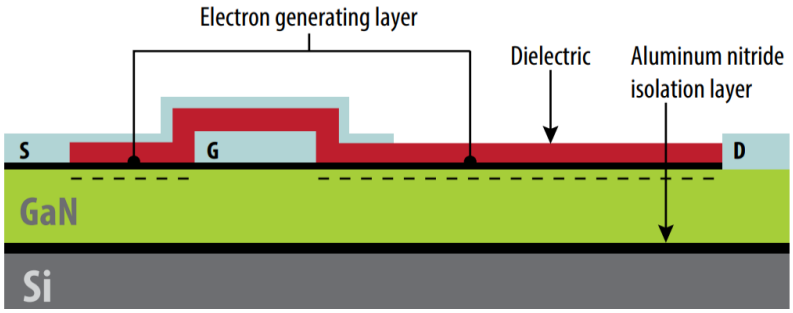

Figure 1.1 GaN power transistor structure

Utilizing already-existing production infrastructure is the first step toward a device's cost effectiveness. Standard CMOS tools are used in EPC manufacturing to produce their devices. The process of EPC starts with silicon wafers. The crystal is converted from silicon to GaN by growing a thin layer of Aluminium Nitride (AlN) on the silicon using a MOCVD reactor. This is a seed layer that is applied to the silicon wafer in order to generate a thick layer of extremely resistant GaN. Wide bandgap materials like GaN can withstand high voltage over short distances. The GaN layer offers the GaN transistor a base upon which to be constructed. A layer of highly conductive Aluminium Gallium Nitride (AlGaN) is deposited, producing a piezoelectric polarization and generating an abundance of electrons just beneath the AlGaN [1].

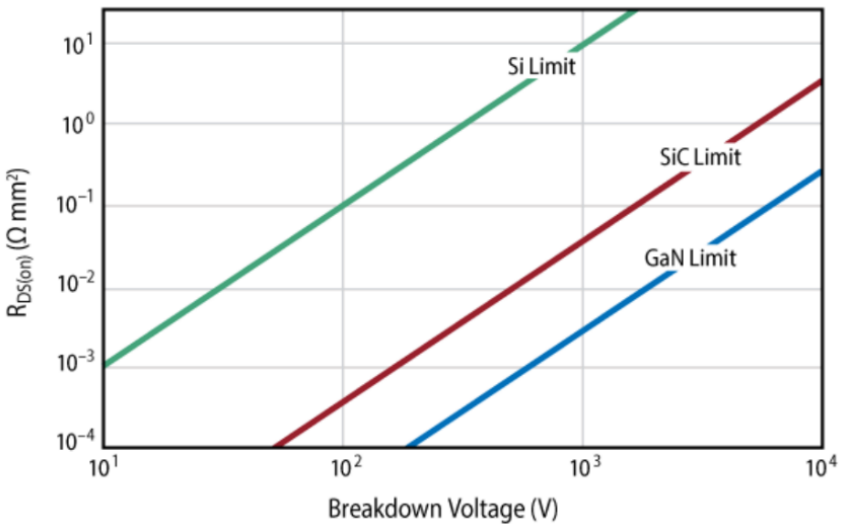

Figure 1.2 Theorical limits of Si, SiC and GaN with related to breakdown voltage

Compared to SiC and Si devices, GaN devices have a significantly lower on-resistance per unit area for the same voltage rating as shown in Figure 1.. This results in a much lower box and die size. Furthermore, from a system viewpoint, GaN's quick switching speed permits greater switching frequencies, which permit a decrease in the size of passive components and, in certain situations, the removal of mechanical heatsinking. When utilizing GaN FETs and ICs, this leads to an overall decrease in the size and weight of the final solution [11].

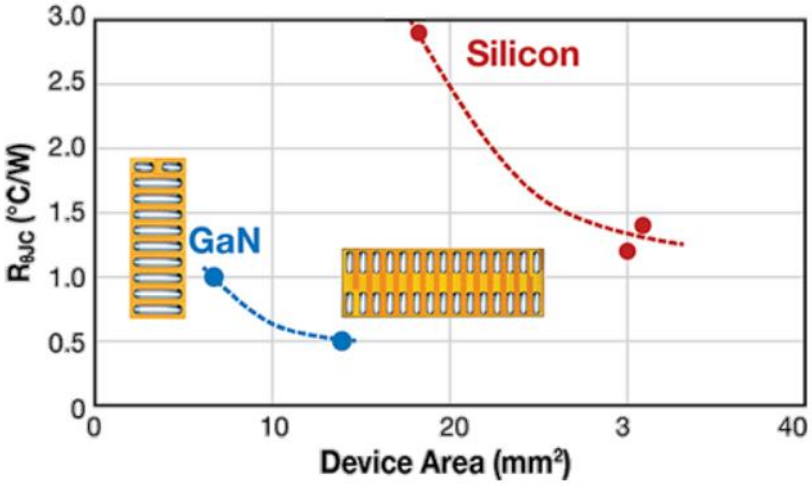

Figure 1.3 Theorical thermal limits of Si and GaN with related to device area

Heat is the result of a device's power consumption during operation. For this reason, it's critical to comprehend how well a device transfers heat to its surroundings. When compared to analogous RDS(on) MOSFETs, GaN FETs have a substantially lower FET area, but they nevertheless have good absolute thermal performance. The junction-to-case path of chip-scale GaN transistors offers good thermal conductance since their thermal resistance to case (RθJC) is actually lower than that of silicon devices [11].

1.1.2 Silicon Fets

Field-Effect Transistors (FET’s) are essential components in modern electronics, widely used for their ability to control electrical current flow with high efficiency and low power consumption. FETs, including junction FETs (JFETs) and

metal-oxide semiconductor FETs (MOSFETs), function by using an electric field to modulate the conductivity of a semiconductor channel. This modulation capability makes FETs ideal for amplifying or switching electronic signals in a vast array of applications, from microprocessors to power management systems. According to a study published by the Institute of Electrical and Electronics Engineers (IEEE), FETs are crucial for the development of low-power electronics due to their high input impedance and fast switching capabilities [12]. Additionally, the International Roadmap for Devices and Systems (IRDS) highlights that advancements in FET technology, particularly the scaling of MOSFETs, are central to the continued progress of semiconductor miniaturization and performance enhancement [13]. These attributes underline the importance of FETs in driving innovation and efficiency in electronic devices.

1.1.3 SiC Fets

Silicon Carbide (SiC) Field-Effect Transistors (FETs) are advanced semiconductor devices renowned for their high efficiency and performance in power electronics. SiC FETs outperform traditional silicon transistors by offering higher thermal conductivity, greater breakdown voltage, and faster switching speeds, making them ideal for high-power and high-frequency applications. These attributes significantly enhance the performance of electric vehicles, renewable energy systems, and industrial power supplies. The higher efficiency and reduced cooling requirements of SiC FETs contribute to smaller, lighter, and more energy-efficient power systems. For instance, a study by Wolfspeed indicates that SiC devices can achieve up to a %50 reduction in power losses compared to silicon counterparts [14]. Additionally, research from Yole Développement highlights that the SiC market is projected to grow at a compound annual growth rate (CAGR) of %30 through 2026, driven by their adoption in electric vehicles and industrial applications [15]. These advancements underscore the critical role of SiC FETs in modern electronics, paving the way for more robust and efficient power management solutions.

1.2 Buck-Boost Converters

Buck-boost converter topologies are essential in power electronics for applications requiring voltage conversion either above or below the input voltage. These converters can efficiently manage the power supply in various electronic systems. Here is a list of common buck-boost converter topologies:

1.2.1 Non-Inverting Buck-Boost Converter

Combines buck and boost modes to produce an output voltage that can be either higher or lower than the input voltage, but always with the same polarity. Suitable for low power applications [16]. Compatible to work with high switching frequencies. [17]. Non-linear relationship between duty cycle and output voltage. But, high output ripples Excessive duty cycle ratio is required for higher voltage gain, discontinuous output current properties are disadvantages of the topology [18].

1.2.2 Inverting Buck-Boost Converter

Also known as the conventional buck-boost converter, this topology inverts the polarity of the output voltage while stepping it up or down. The topology uses less switching elements than non-inverting buck boost converter but it uses a diode [19]. Because of forward voltage of the diode the efficiency of the topology is decrease [20].

1.2.3 Sepic (Single-Ended Primary-Inductor Converter)

Provides a non-inverted output voltage and can either step up or step down the input voltage, with the advantage of continuous input current [21]. Non-inverting output. Utilized for power factor correction in AC lines Non-linear relationship between duty cycle and output voltage [22]. Difficult to control duty cycle for multi-input and multi-output configuration. Poor voltage gain duty cycle imbalance for effective operation the on time must be greater than off time in order to get higher output voltage [23].

1.2.4 Zeta Converter

Similar to the SEPIC, it provides a non-inverting output and allows both step-up and step-down voltage conversion, with the advantage of continuous output current [24]. Suitable for medium and high-power applications, non-inverting output but non-linear relationship between duty cycle and output voltage. Also the topology has medium complexity, easy to control, smaller in size and cost effective[25].

1.2.5 ĆUK Converter

Suitable for low power applications It uses capacitor for power transfer and energy storage Non-linear relationship between duty cycle and output voltage [26]. Negative output polarity with respect to input. Efficiency is reduced in multiple output network [27], complex compensation circuitry is required to operate the converter properly, discontinuous output current that is uncontrolled due to resonance of L-C pair, that leads to excessive voltage across capacitor which can damage the circuit [28].

Table 1.1 Comparison of buck-boost converter topologies

Topology	**Advantage**	**Disadvantage**
Non-Inverting Buck-Boost	Simple Configuration, fewer passive components, non-reversed polarity	Non-isolated output, more active components causes higher cost
Inverting Buck-Boost	Simple Configuration, fewer components, higher reliability	Large Input Output current ripples, Inverted output voltage, low efficiency
Sepic	Zero-Ripple output currents by coupling the two inductors, non-reversed polarity	Large inrush current, more component higher weight and size
Zeta	Lower voltage of capacitor, non-reversed polarity, zero ripple output currents by coupling the two inductors.	Larger voltage stress for active components more component higher weight and size
ĆUK	Continous input and output currents zero ripple output current	Large size of L, larger voltage and current reversed output polarity

Table 1.2 Component count and efficiency comparison of buck-boost topologies

Converter type	**Capacitors**	**Switches**	**Diodes**	**Efficiency**	**Output Power**	**References**
Non-Inverting Buck-Boost	1	4	0	%96	500 W	[29]
	1	4	0	%97.5	5 kW	[30]
	1	4	0	%96.7	30 kW	[31]
Buck-Boost	1	2	2	%90.9	150 W	[32]
ĆUK	2	1	1	%90	17 W	[33]
	5	3	6	%94	2 kW	[34]
	2	4	3	%80	125 W	[35]
SEPIC	2	2	3	%95	1 kW	[36]
	5	1	4	%94	600 W	[37]
	2	2	6	%93.5	245 W	[38]
ZETA	6	1	3	%94	300 W	[39]
	2	2	3	%86	30 W	[40]

As Shown in Table 1.1 and Table 1.2 the Non-Inverting Buck-Boost converter offers several advantages, including high efficiency, wide input voltage range, and the ability to maintain a stable output voltage regardless of fluctuations in the input. However, a significant drawback of this converter is the number of switches required, which can complicate the design and increase the overall size of the circuitry. This issue can be addressed by employing small-area, high-power Gallium Nitride (GaN) FETs, which enable higher power density and more compact designs, thereby mitigating the disadvantages associated with the traditional switch-heavy configuration.

1.3 Control Methods

1.3.1 PI Controller

Proportional-Integral (PI) control is a fundamental feedback control strategy widely used in various industrial and engineering applications for maintaining process variables at desired setpoints. PI controllers combine two control actions: proportional control, which responds to the current error between the setpoint and the process variable, and integral control, which addresses the accumulation of past errors. The proportional component provides an immediate corrective response to errors, while the integral component eliminates steady-state errors by adjusting the control output based on the cumulative error over time. This combination results in a control system that is both responsive and accurate. According to a study by the International Society of Automation (ISA), PI control is particularly effective in systems where precise control is necessary but derivative action, which responds to the rate of change of the error, is not required or may introduce excessive noise [41]. The simplicity and robustness of PI controllers make them a popular choice for regulating processes in industries such as chemical manufacturing, HVAC systems, switch mode power supplies and motor speed control.

1.3.2 One Cycle Control (OCC)

One-Cycle Control (OCC) algorithm is an advanced control method used in power electronics to achieve precise regulation of power converters by ensuring that the average value of a control variable over each switching cycle matches a desired reference. This technique is particularly effective in reducing harmonics and improving the dynamic response of power converters. OCC operates by adjusting the duty cycle within each switching period to force the integral of the error signal to zero, thus achieving instantaneous control and maintaining the desired output. Research published in the IEEE Transactions on Power Electronics highlights the effectiveness of OCC in applications such as inverters and rectifiers, demonstrating its ability to provide fast transient response and high efficiency under varying load conditions [42]. Additionally, studies from the Journal of Power Electronics indicate

that OCC's simplicity and robustness make it suitable for a wide range of power conversion applications, including renewable energy systems and electric vehicle chargers [43]. The algorithm's capability to minimize switching losses and improve power quality makes it a valuable tool in modern power electronics design.

1.3.3 Sliding Mode Control (SMC)

Sliding Mode Control (SMC) is a robust and adaptive control strategy widely used in nonlinear systems and applications requiring high performance under varying conditions. SMC operates by forcing the system state to "slide" along a predetermined surface, known as the sliding surface, by applying a discontinuous control signal. This method offers several advantages, including insensitivity to system parameter variations and external disturbances, which enhances the system's stability and performance. According to a study published by the International Journal of Control, Automation, and Systems, SMC is particularly effective in handling uncertainties and non-linearities, making it ideal for applications such as robotics, automotive systems, and power electronics [44]. Additionally, research from IEEE Transactions on Industrial Electronics highlights that SMC's ability to maintain robust performance in the face of model inaccuracies and external perturbations is crucial for advanced control systems in aerospace and industrial automation [45]. The inherent robustness and adaptability of SMC ensure its continued relevance and application in modern control engineering.

CHAPTER 2

METHODOLOGY

2.1 Circuit Description and Operation

The bi-directional non-inverting buck-boost converter is simply a combination of a buck converter and boost converter. As shown in Figure 2.1. there are two parts, the buck section of the topology, decreases the input voltage. The boost part of the circuit increases the voltage which is generated from the buck side and transfers it to the output. To increase efficiency of the switch Q2 and Q3 components selected as switching devices instead of diodes.

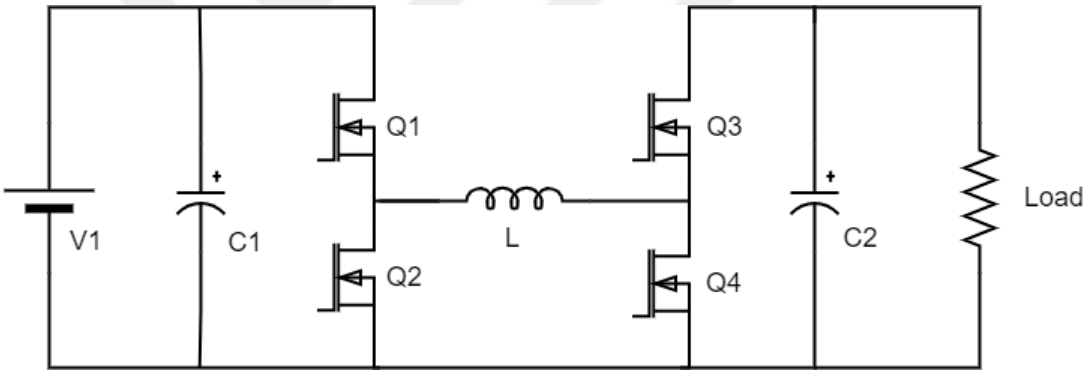

Figure 2.1 Non-inverting buck-boost converter topology

2.1.1 Operation of Buck Mode

The buck mode of the circuit consists of 2 stages: inductor charging stage and discharging stage. The operation of buck stage1 is given in Figure 2.2

Buck Stage 1: The current starts with turning on the Q1&Q3 and turning off Q2&Q4 switches. In this stage the inductor L charges. The voltage dropped on L and the output voltage are explained by the following equations.

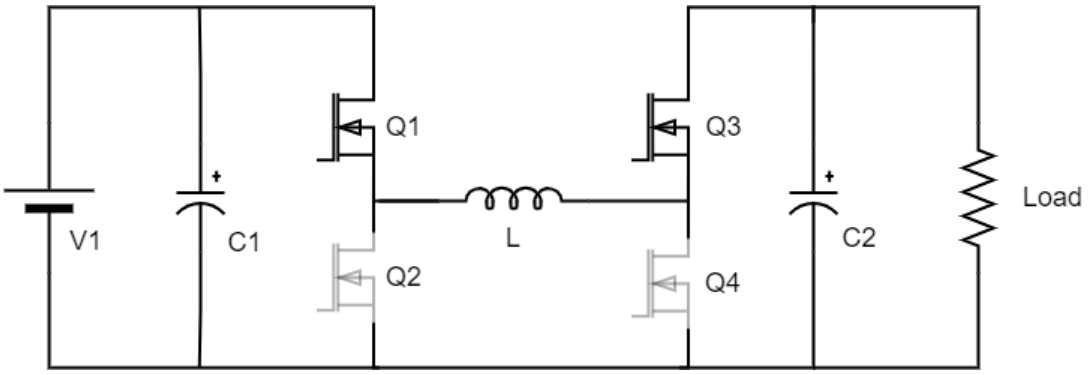

Figure 2.2 Operation of buck stage 1

$$V_{L1} = L_1 * \frac{di}{dt} \quad \textbf{(2.1)}$$

$$V_{OUT} = V_{IN} - V_{L1} \quad \textbf{(2.2)}$$

Buck Stage 2: During stage 2 the Q2&Q3 switch turns on and Q1&Q4 switches turns off. The Charged inductor L in previous stage, will changes the polarity and supply the required output voltage. During this stage output power supplied by C2 and L components. The voltage supplied by L and output voltage is explained by the following equations.

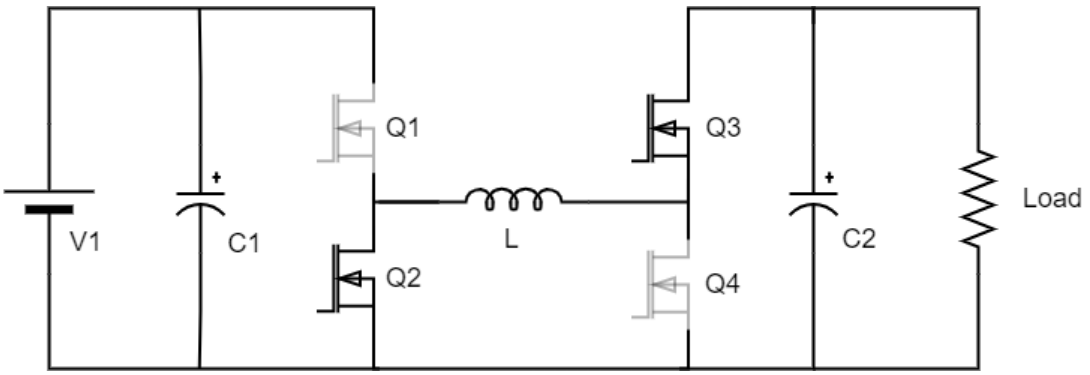

Figure 2.3 Operation of buck stage 2

$$V_{L1} = V_{OUT} \quad \textbf{(2.3)}$$

$$V_{L1} = L * \frac{di}{per(1-D)} \quad \textbf{(2.4)}$$

Substitute Equation (2.4) in Equation (2.3)

$$di = V_{OUT} * \frac{per(1-D)}{L} \quad \textbf{(2.5)}$$

To calculate relation between inductor voltage, output voltage and duty substitute Equation (2.5) in Equation (2.3)

$$V_{L1} = V_{OUT} * \frac{1-D}{D} \quad \textbf{(2.6)}$$

To calculate input voltage, output voltage and duty relation for buck mode substitute Equation (2.6) in Equation (2.2)

$$V_{OUT} = V_{IN} * D \quad \textbf{(2.7)}$$

During Buck operation Q4 switch remains turned off and Q3 switch turned on, the main reason Q3 turned on is to be getting rid of Q3's body diode forward voltage and increase the efficiency of the circuit.

2.1.2 Operation of Boost Mode

The boost mode of the circuit consists of 2 stages: inductor charging stage and discharge stage.

Boost Stage 1: During stage 1 the Q1&Q4 switch turns on and Q2&Q3 switches turns off. In this stage the inductor L charges. The voltage on L and the output voltage are explained by the following equations.

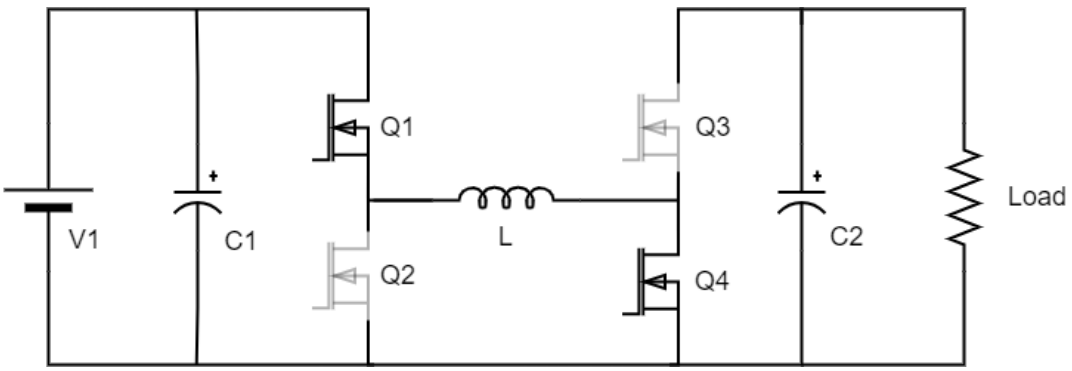

Figure 2.4 Operation of boost stage 1

$$V_{L1} = L_1 \frac{di}{dt} \quad \textbf{(2.8)}$$

$$V_{L1} = V_{IN} \quad \textbf{(2.9)}$$

Boost Stage 2: During stage 2 the Q1&Q3 switch turns on and Q2&Q4 switches turns off. The charged inductor L in previous stage, will change the polarity and connected series with input voltage, by addition the input voltage and L inductor voltage, the circuit supplies required output voltage. During this stage output power is supplied by C2 and L components. The voltage supplied by L, and output voltage is explained by the following equations.

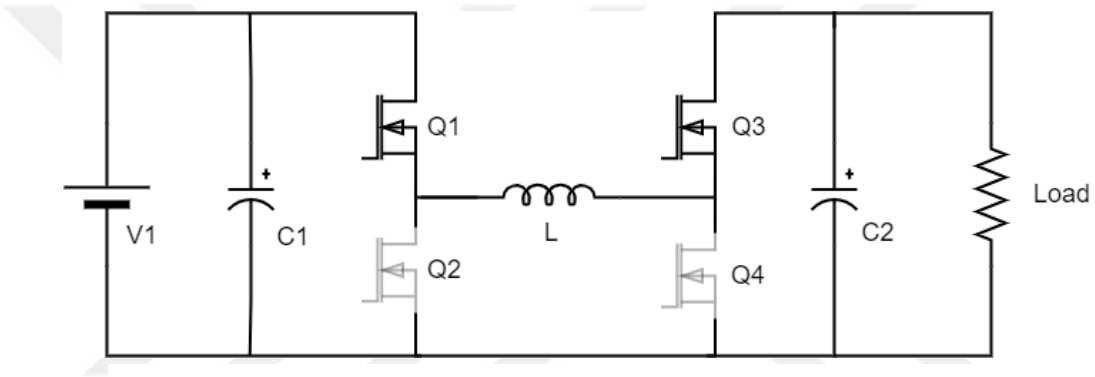

Figure 2.5 Operation of boost stage 2

$$V_{OUT} = V_{IN} + V_{L1} \quad \textbf{(2.10)}$$

To calculate the relation between input voltage, output voltage and duty for boost operation, substitute Equation (2.9) in Equation (2.8) and Equation (2.8) in Equation (2.10)

$$V_{OUT} = \frac{V_{IN}}{1-D} \quad \textbf{(2.11)}$$

2.1.3 Calculation of Passive Components

According to technological developments in semiconductor technologies, the switching frequencies of switching components are increased. In this paper, the switching frequency is selected as 500 kHz. Increasing the switching frequency allows the passive elements to shrink in size. By using this benefit, it can be designed higher power density and more compact modules.

L is selected for %25 ripple current (4A) for maximum current (16A), Maximum output voltage 40V and minimum input voltage 10V.

For 10V input and 40V output;

$$40 = \frac{10}{1-D} \Rightarrow D = 0.75 \quad \textbf{(2.12)}$$

Substitute these values in Equation (2.8) and Equation (2.9)

$$40 = L_1 * \frac{16}{0.75*2*10^{-6}} \Rightarrow L=3.75uH \quad \textbf{(2.13)}$$

The closest commonly used value for inductor is 4.7 uH so 4.7 uH inductor selected for simulation.

C1 Selected for 1V voltage ripple or less

$$dV = \frac{dt*Iout}{C1} \quad \textbf{(2.14)}$$

$$C1 = \frac{per*D*Iout}{dV} \quad \textbf{(2.15)}$$

$$C1 = \frac{2*10^{-6}*0.25*40}{1} \Rightarrow C=20uF \quad \textbf{(2.16)}$$

The closest commonly used value for capacitor is 22 uF so 22 uF capacitor selected for simulation and experimental studies.

2.2 Control Method of Proposed Topology

A bidirectional DC-DC converter is a power electronic device that facilitates the seamless transfer of electrical energy between two DC voltage sources bidirectionally. This converter operates in both step-up (boost) and step-down (buck) modes, allowing it to efficiently regulate voltage levels in both directions. The PI control method is adopted to regulate output voltage and limit the output current. The PI controller uses an error input and gives a duty output. The error is multiplied by a proportional constant (K_P) and integrated with a constant (K_I). The output is the sum of multiplication and integration for the PI block. Then, the output of the block is given to a saturation block, which defines the maximum and minimum output current. If the output current exceeds the saturation limits, the output of the PI is saturated. In this way, the input of the current PI controller decreases, then the output voltage, and limits the output current.

The bidirectional functionality is particularly useful in applications such as energy storage systems, electric vehicles, and renewable energy systems where energy needs to be efficiently transferred between different voltage levels. In the step-up mode, the converter boosts the voltage from a lower input level to a higher output level, while in the step-down mode, it reduces a higher input voltage to a lower output voltage. There is a voltage command where the PI controller references the voltage value to determine the output voltage regardless of the input voltage. In this paper, bidirectional working is performed by the relation between commanded voltage and load voltage: if the load voltage is lower than the commanded voltage, the energy flows from input to output. If the load voltage becomes greater than the commanded voltage, the energy flows from output to input.

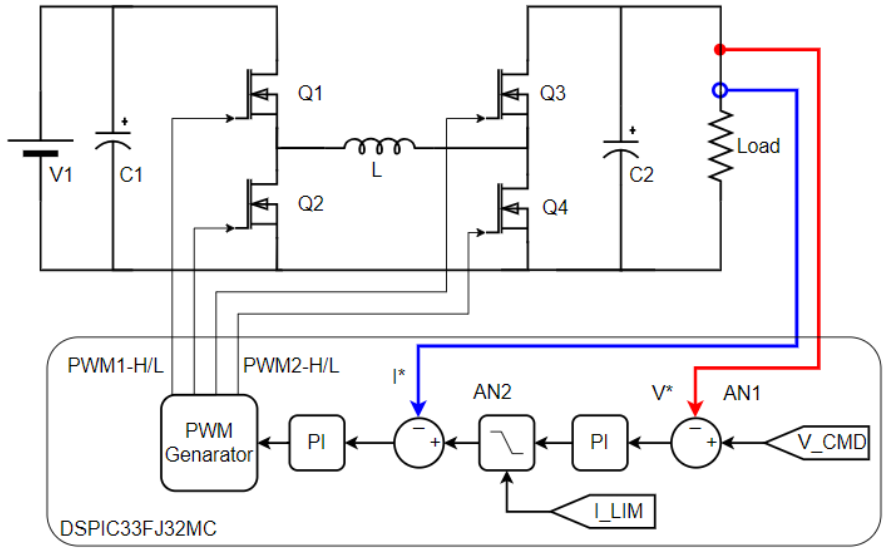

Figure 2.6 Block diagram of control strategy of proposed topology

The controller's output is saturated between %0 and %170, giving us the ability to use only one controller for both buck and boost modes. The output of the controller is directly connected to the duty input of the buck converter. The input of the buck converter is saturated after %95, duty, and the boost converter's input is also saturated when the output of the PI controller is less than %95. When the PI controller's output is above %95, the circuit starts to decrease the duty of the boost converter side; in this way, the output current can be regulated.

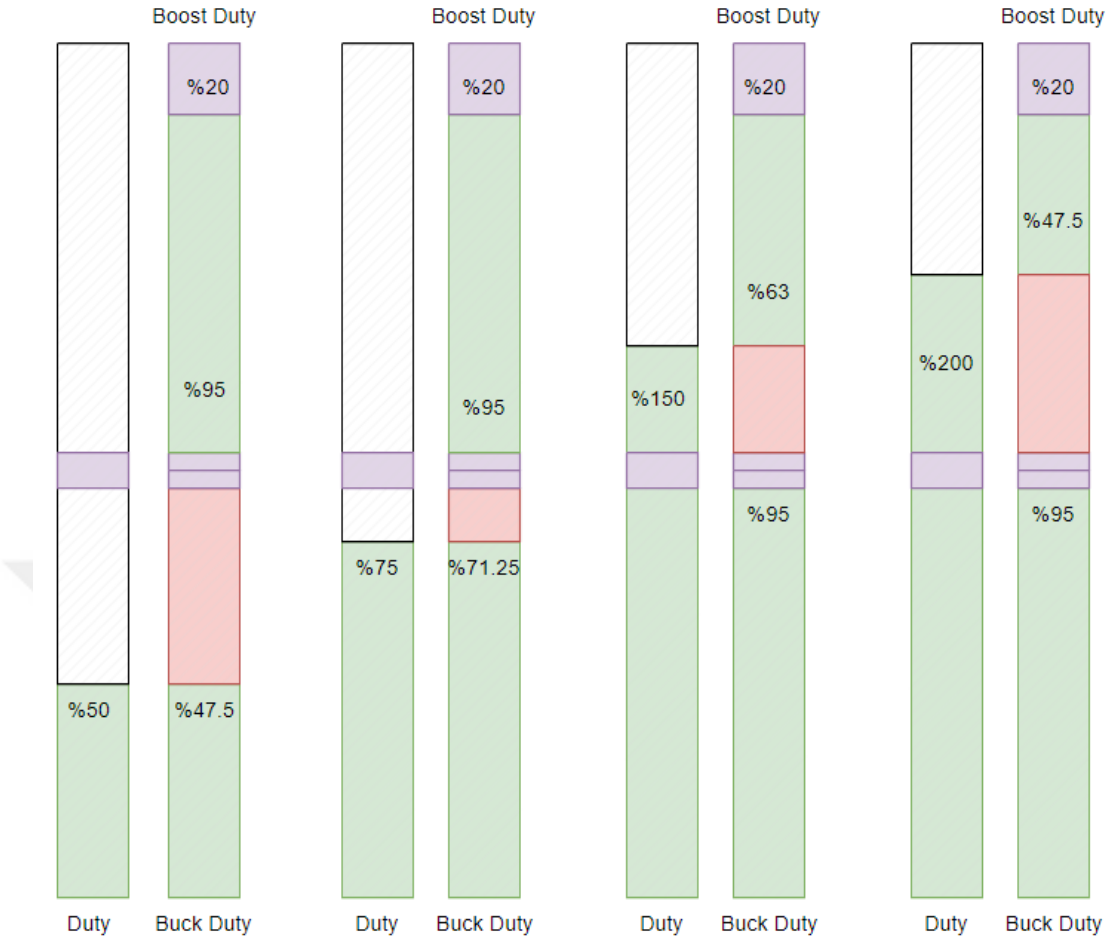

Figure 2.7 Relation between control duty command and buck-boost PWM duty

The duty that calculated from PI output is illustrated in duty column. buck and boost duty is shown in a same column, upper half of the column shows boost duty, lower half of the column shows buck duty. The Figure 2.7 shows how a single PI output control the device's both buck and boost duties. By this way one single duty command can drive both buck and boost side switches.

2.3 Simulation Studies

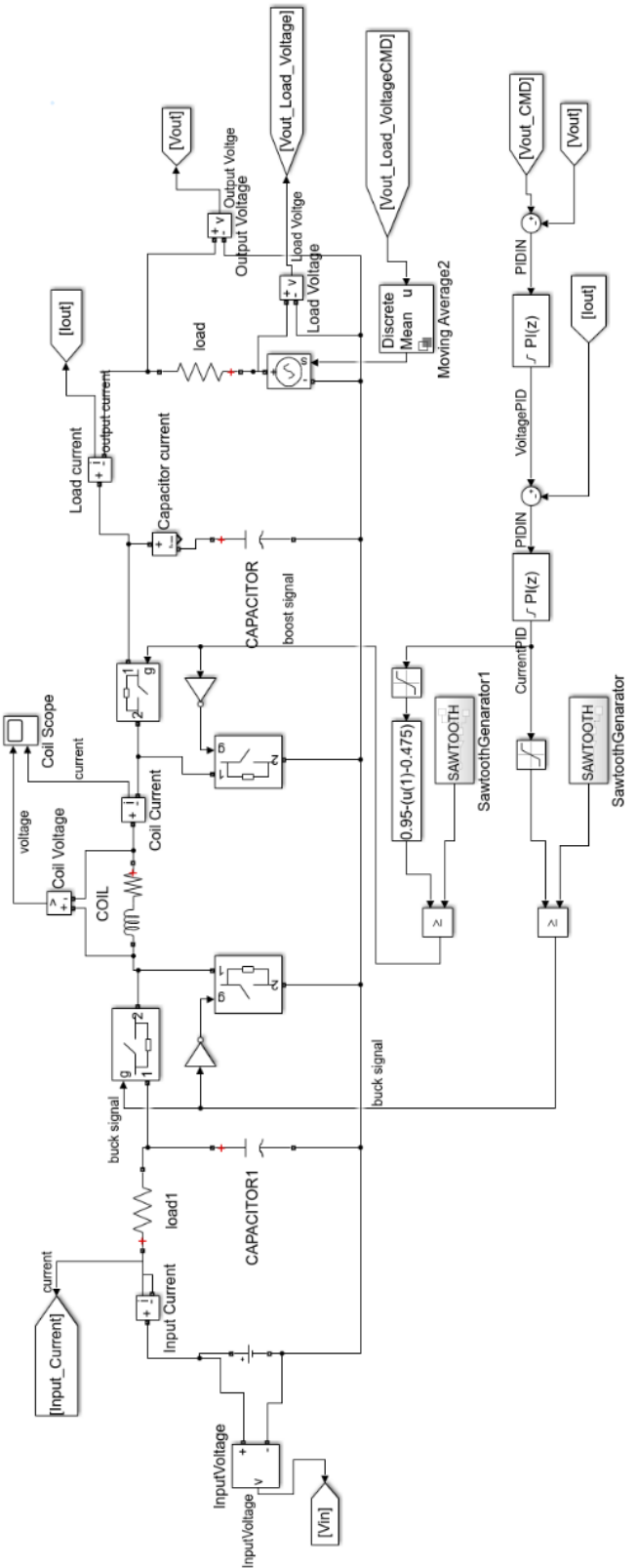

Figure 2.8 Implementation of control method to proposed topology

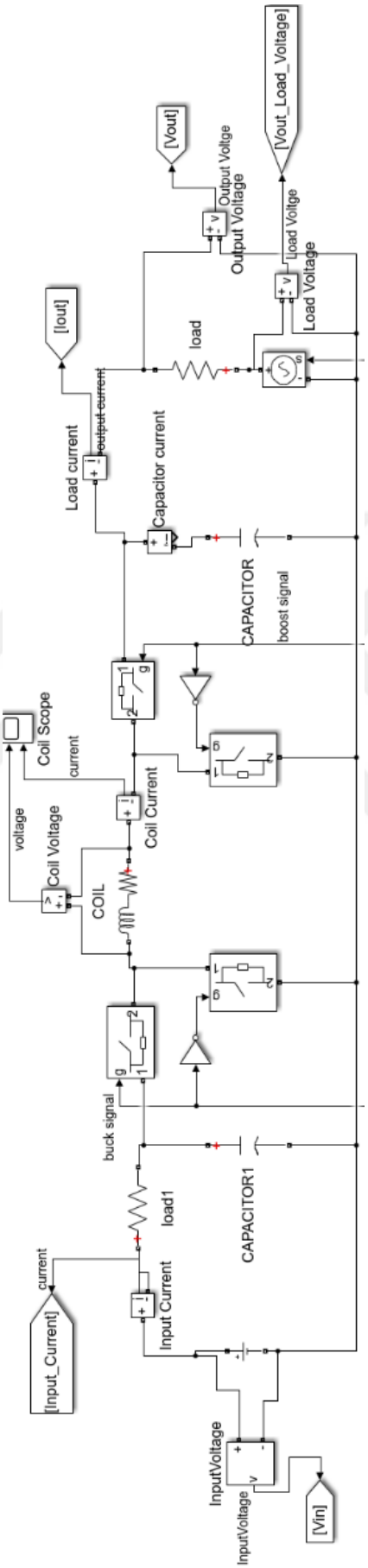

Figure 2.9 Power circuit of matlab simulation

In Figure 2.8, it is seen a voltage source at the input, then a non-inverting buck-boost topology as explained before, and a load. The load contains two components: a resistor and an adjustable voltage source. The adjustable voltage source represents a dynamic load that both consumes and produces energy. We can use an electric car as an example to define a dynamic load. When the car accelerates, the load consumes energy from the batteries; when the car brakes, the load produces energy and charges the batteries. The resistor represents system impedance.

2.4 Hardware Scematic Design

Bi-directional non-inverting buck-boost converter design, which was previously explained and calculated, was made with using the program called Altium Designer. The circuit design consist of six schematics

1. Main sheet:

The Main sheet is shown in Figure 2.10 includes five other schematics. It shows the relation of other sheets and shows the flow of the hardware. The power comes from input connectors and then goes on power stage of the circuit. The output of the power stage is connected both Measurements and Output filter. The Measurement schematic measures output voltage and current to provide voltage feedback to MCU and output filter, filters the output voltage to eliminate output noises.

2. Power Stage:

The Power Stage is shown in Figure 2.11 consists of four GaNFET's and two boostrap gate drivers. The Gan Fets used in this schematic is "EPC2065" manufactered by EPC (Efficient Power Conversion) company. It has 80V maximum Drain-Source voltage and 60A maximum continous current drive capability with 3.6 m Ω Drain-Source resistance. To drive half bridge GaN FET's "Up1966E" 80V half bridge gate driver is used. The boostrap gate driving technique is very useful for driving high side switch in a small area. As shown in Figure 2.11 R1, R5, R10, R17 and C2, C6, C8, C12 components is used for designing snubbers to reduce MOSFET's voltage stress. L1 is the main power coil for Bi-directional non-inverting buck-boost converter topology. The coil is 4.7 uH with 5.5 mΩ dc resistance and

25A continuous current capacity. Coil's main material is Chernobyl powdered code and Self Resonance frequency is 15Mhz so it makes the coil is suitable for high frequency applications. The coil has shielded construction so we can use is near of the analog measurement units without signal distortion.

3. Measurements:

The measurements schematic is shown in Figure 2.12. There are three voltage dividers on this schematics, the voltage divider made with R30 and R32 is to give output voltage feedback to MCU. The voltage divider made with R31 and R34 is to give input voltage feedback to MCU. The voltage divider made with R29 and R33 is to give temperature feedback to MCU, the R33 resistor is a NTC. U6 component is an operational amplifier to amplify the output current sensed by R26 shunt resistor, with an 1.65V offset to measure bidirectional current. The output current of the device is pass through R26 "10 mΩ" resistor. For 1A current the voltage on the R26 resistor is 1A*10 mΩ = 10 mV. The U6 has 5/1 gain and 1.65V offset, so the output voltage will be 1.65V + 5*10mV = 1.70V. By this way we can measure up to ± 33A output current. The power dissipated on the resistor at 10A is 10*10*0.01 = 1 watt so the output resistance is capable of drive 10A continous current on it.

4. MCU:

The MCU schematic is shown in Figure 2.13. The schematic consist of an MCU and its peripheral components. The MCU that used in bi-directional non-inverting buck-boost converter is "DSPIC33FJ16GS502". The MCU has high-performance 16 bit architecture capable of work 40MIPS speed. The MCU has an ADC peripheral with 6 channel, 10 bit 4 MSPS PWM-Syncronisation and has an PWM peripheral with 4 channel 1.04 ns resolution programmble deadtime. Also the MCU has programmble pin mux option it provides the MCU select programming pins as UART (12.5 Mbps), I2C(1Mbps with SMBus) or SPI communications. The MCU has also an internal oscilator but in this design an external crystal oscillator selected to minimize frequency variation caused for temperature changes.

5. Output Filter:

The Output Filter schematic is shown in Figure 2.14 The circuit is provide a LC filter. There are two 470nH Ferrite bead is used at output to minimise high frequency switching noises. The self resonance of the Inductor is 100 Mhz so it makes the coil is suitable for high frequency filtering. The output capacitor is selected a low ESR and ESL ceramic capacitor so it also aims to clean high frequency noises. The Bi-directional non-inverting buck-boost converter is works on constant 500kHz switching frequency but, the switching noises can be occured on much more higher frequencies. It causes analog feedback signal distortions, conducted and radieted emissions which can be very harmfull for other devices and also the device itself. To protect the electronic devices the output filter is very important the component selection and material qualification is essantial to design a good filter.

6. Power Regulation:

The power regulation schematic is shown in Figure 2.15. There is a buck regulator designed with “LM5007” buck converter IC manufactured by Texas Instruments to provide constant 7.5V output with 9V-80V range voltage input. We need to provide a 5V power to supply GaN FET gate drivers and 3.3V power to supply MCU. The switching converter supply constant 7.5V efficiently than 5V and 3.3V is derived from this voltage with using 2 LDO’s. Heat dissipation is considered for this design the maximum working temperature is estimated as 85°C ambient temperature.

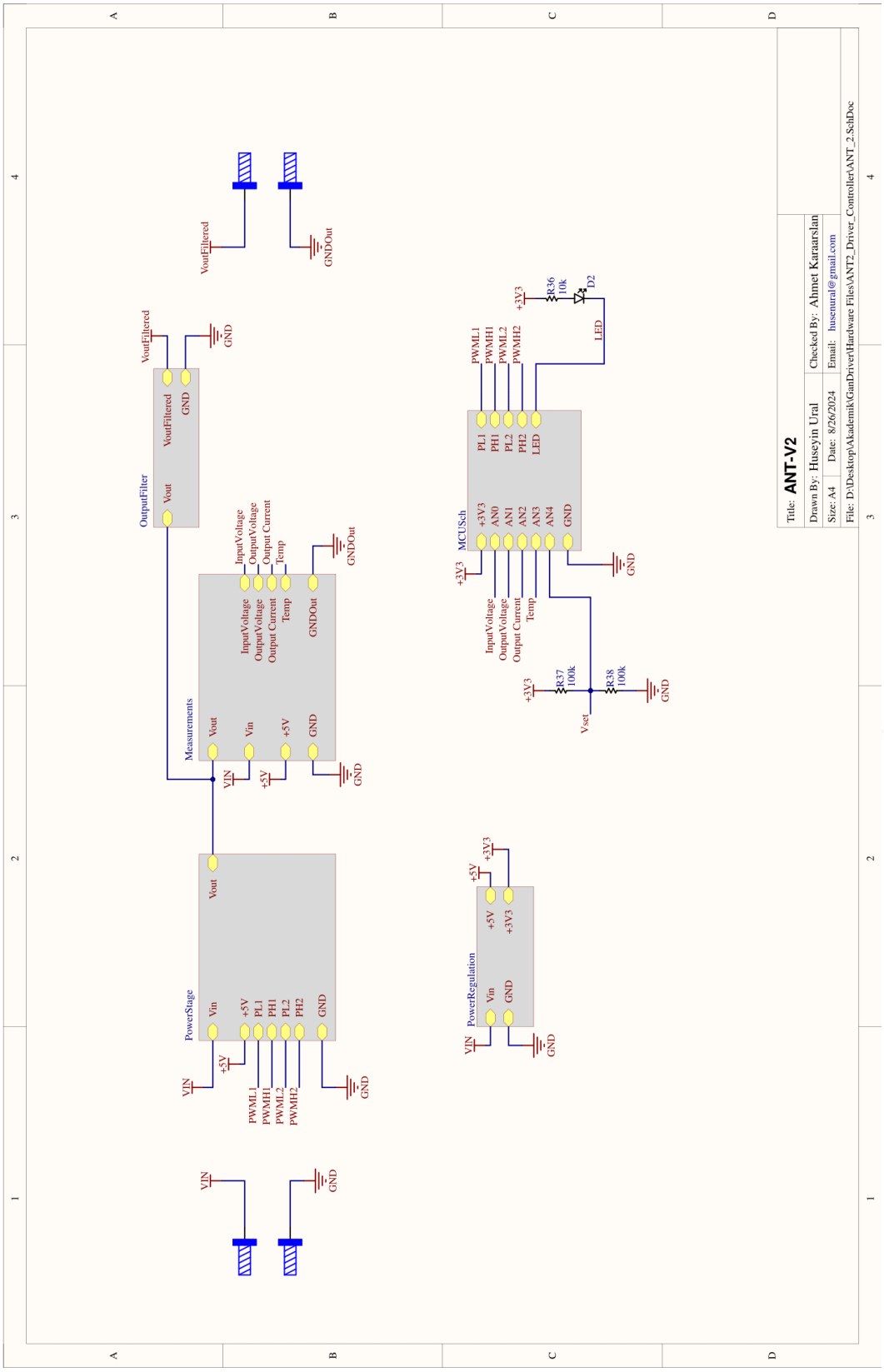

Figure 2.10 Hardware schematics: Main Sheet

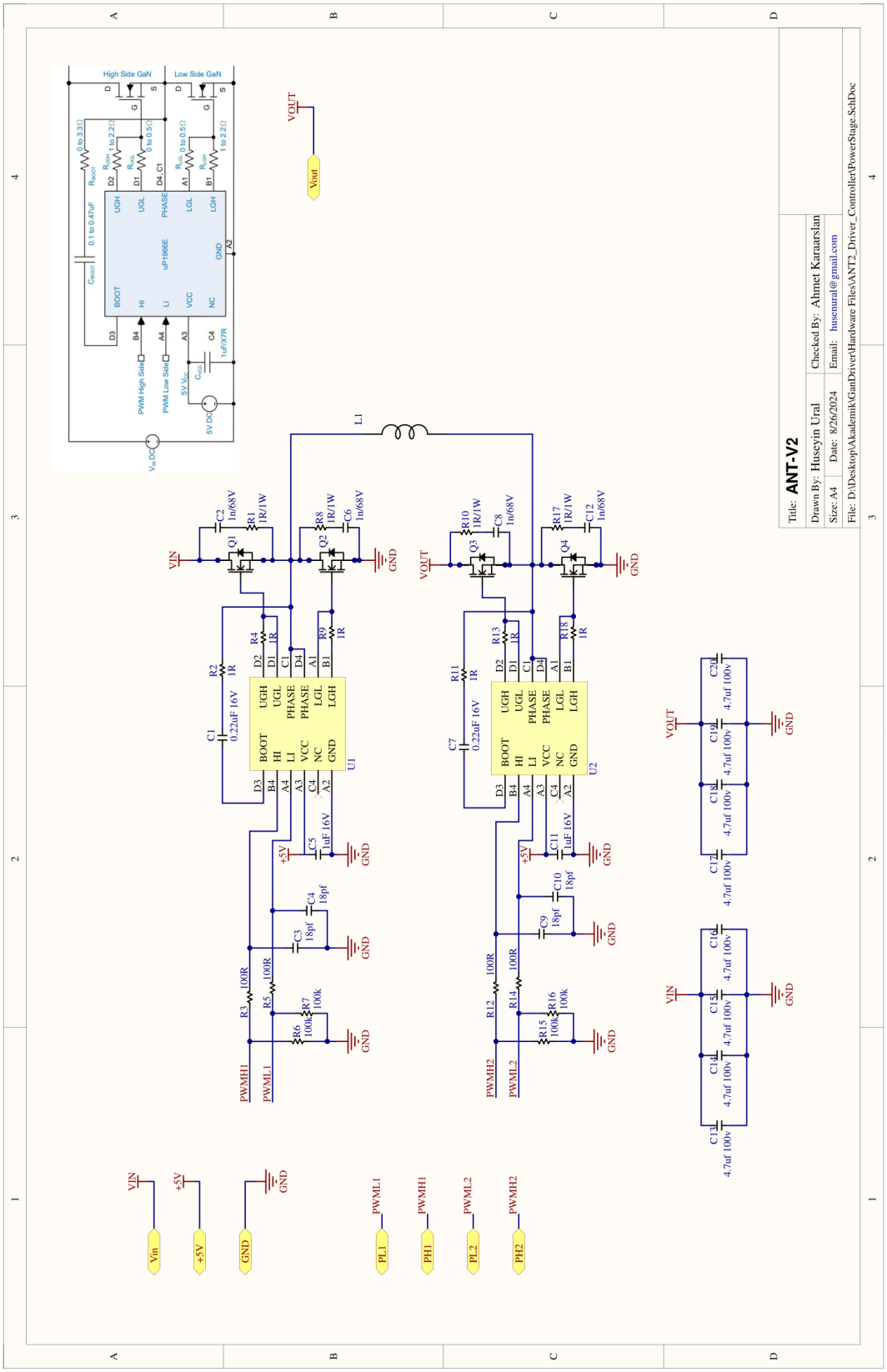

Figure 2.11 Hardware schematics: Power Stage

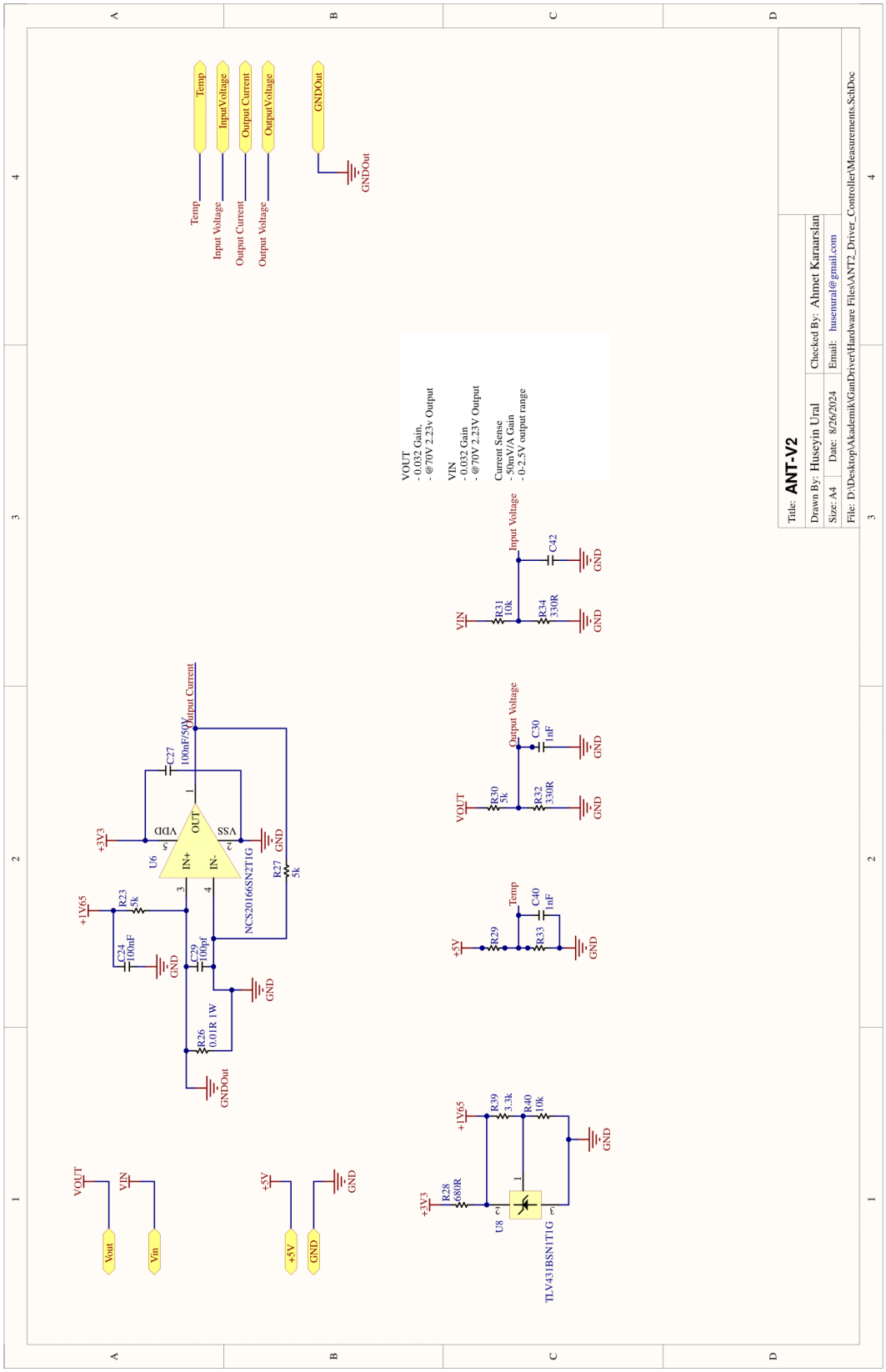

Figure 2.12 Hardware schematics: Measurements

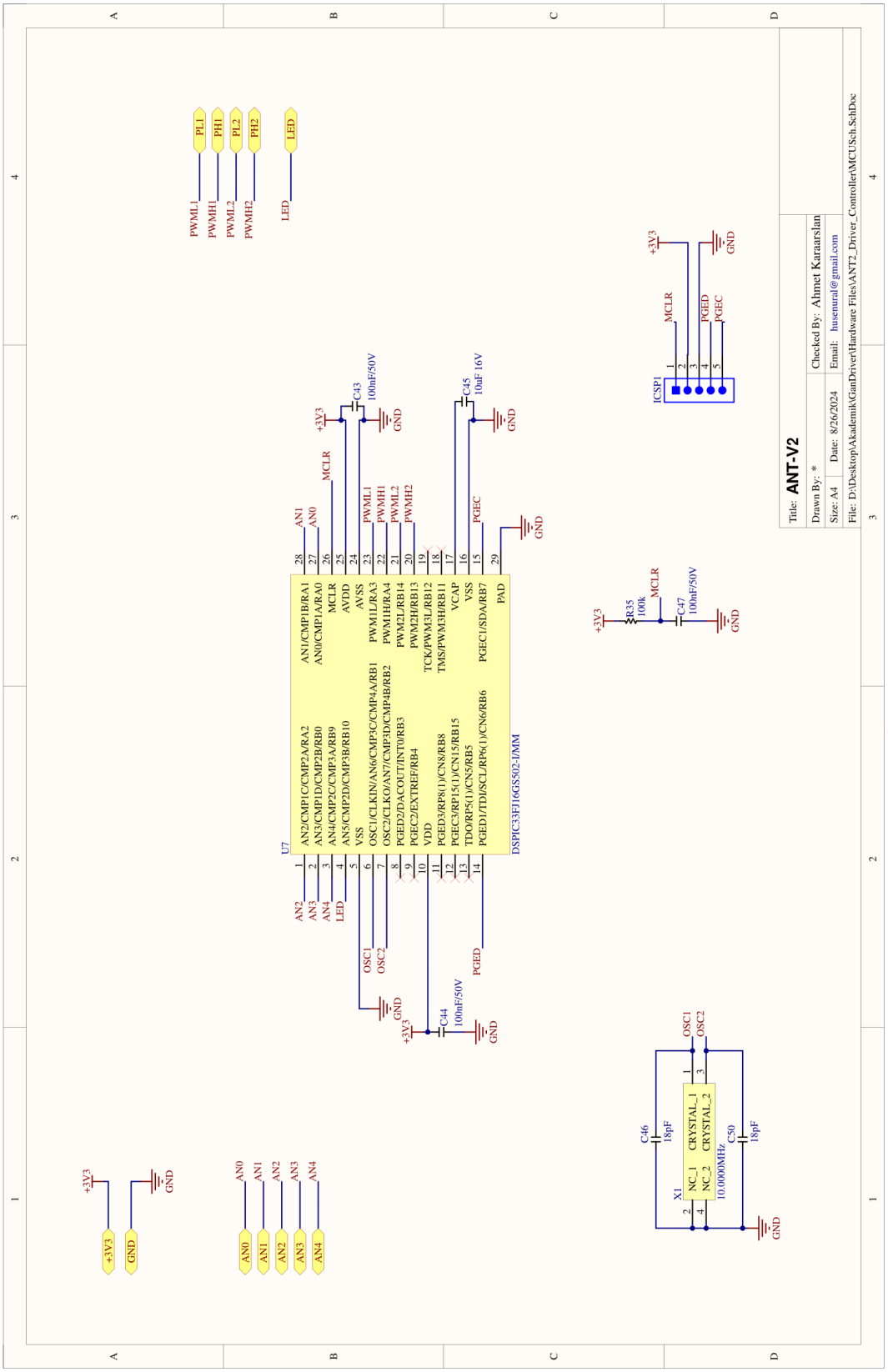

Figure 2.13 Hardware schematics: MCU

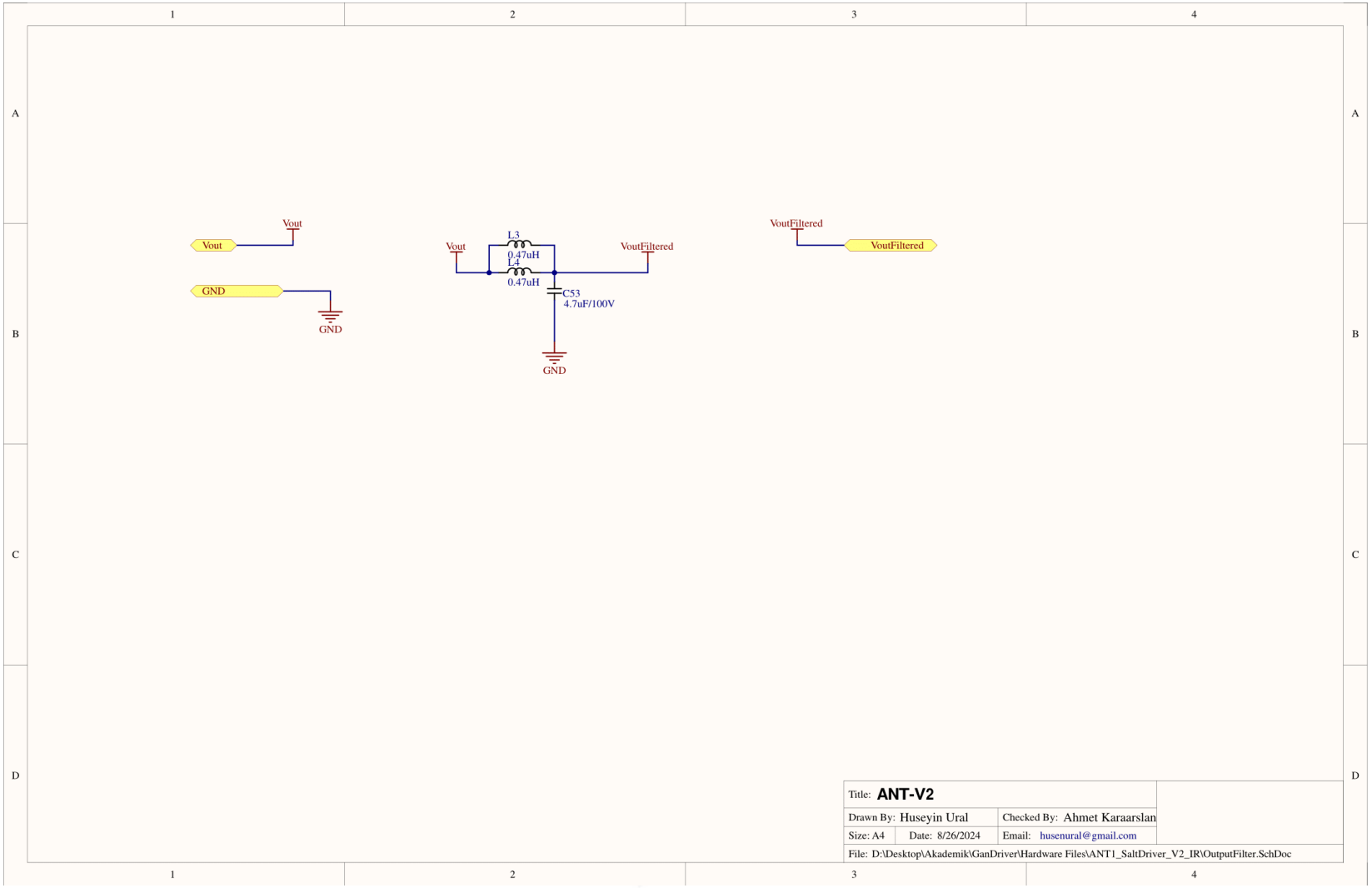

Figure 2.14 Hardware schematics: Output Filter

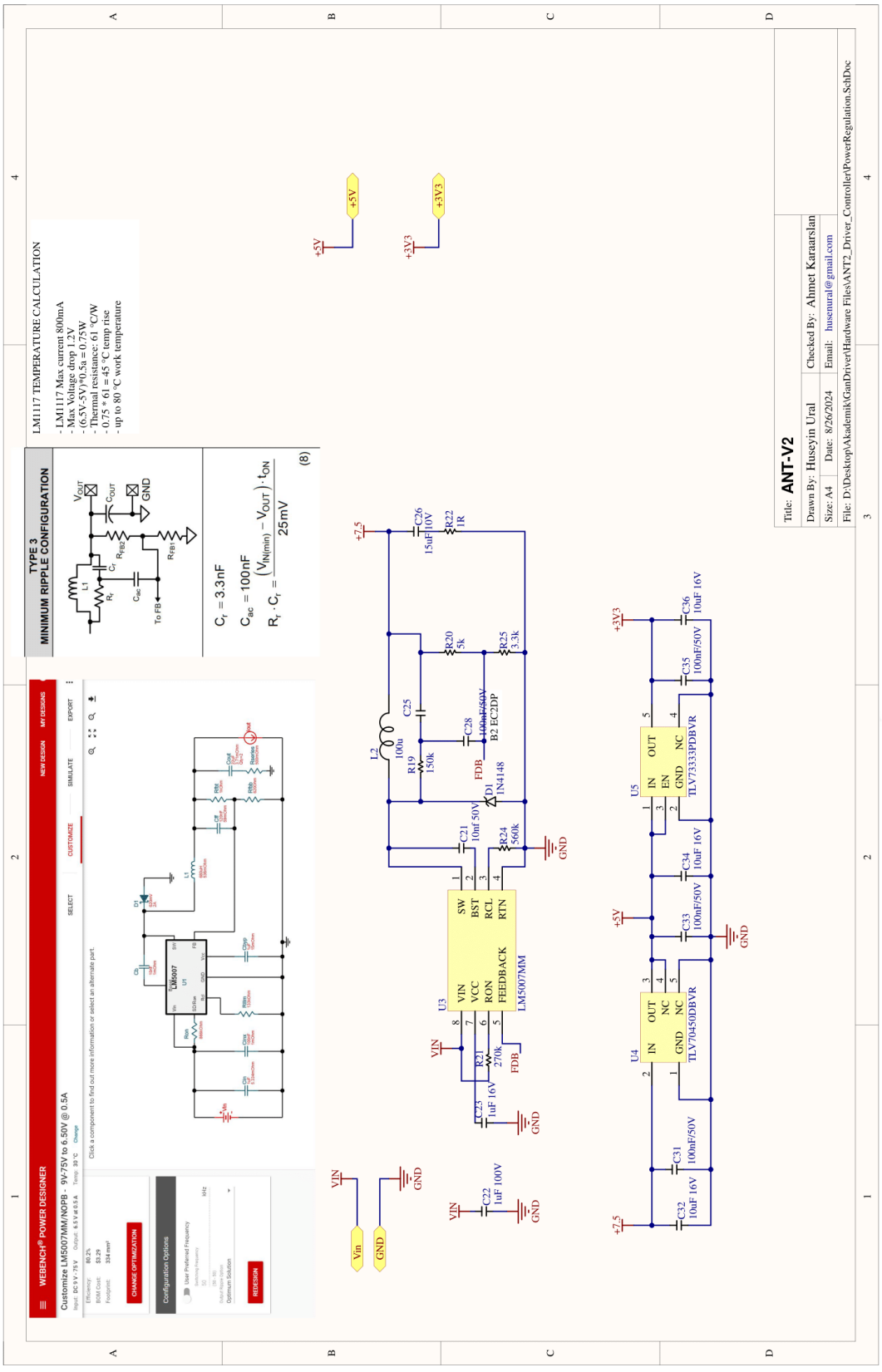

Figure 2.15 Hardware schematics: Power Regulation

2.5 Hardware PCB Design

Printed Circuit Board (PCB) layout design is a critical phase in the development of electronic devices, directly impacting their performance, reliability, and manufacturability. Effective PCB layout design involves the strategic placement of components and routing of electrical connections to ensure optimal signal integrity, thermal management, and electromagnetic compatibility (EMC). Key considerations include minimizing noise and interference, reducing the length of critical signal paths, and ensuring proper grounding and power distribution. Techniques such as layer stacking, trace width optimization, and the use of vias play a crucial role in achieving these goals. According to a study by the Institute of Electrical and Electronics Engineers (IEEE), advanced PCB layout design can significantly enhance the functionality and longevity of electronic systems, especially in high-frequency and high-power applications [46] . Additionally, the increasing complexity of modern electronics, with their higher component densities and faster signal speeds, necessitates sophisticated design tools and best practices to prevent issues such as signal crosstalk and heat dissipation problems. The meticulous design of PCB layouts is thus fundamental to the success of electronic product development, ensuring that devices meet performance specifications and regulatory standards. In this design we create two seperate PCB to use the volume much effectively. The first PCB include MCU , Power Stage, Measurements and Output filter

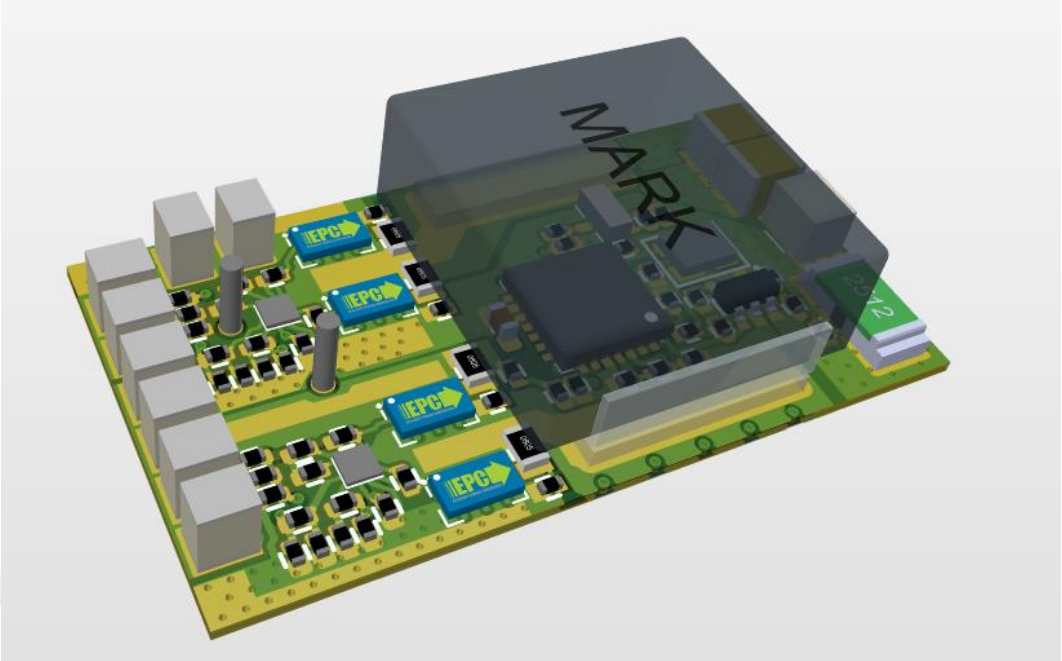

Figure 2.16 Main PCB 3D image

As shown in Figure 2.16 the PCB has been designed vey high denstity the output filter and Input capacitances placed near the components to decrease prasitic Iductance and resistances. MCU placed under the coil and to protect MCU from high noise the coil selected as shielded. Output filter placed at the output of the circuit to eliminate unwanted electrical noise. Down side of the PCB is designed to solder the converter to another PCB. When thinked about size and weight of the device we can easily use it like an surface mount component.

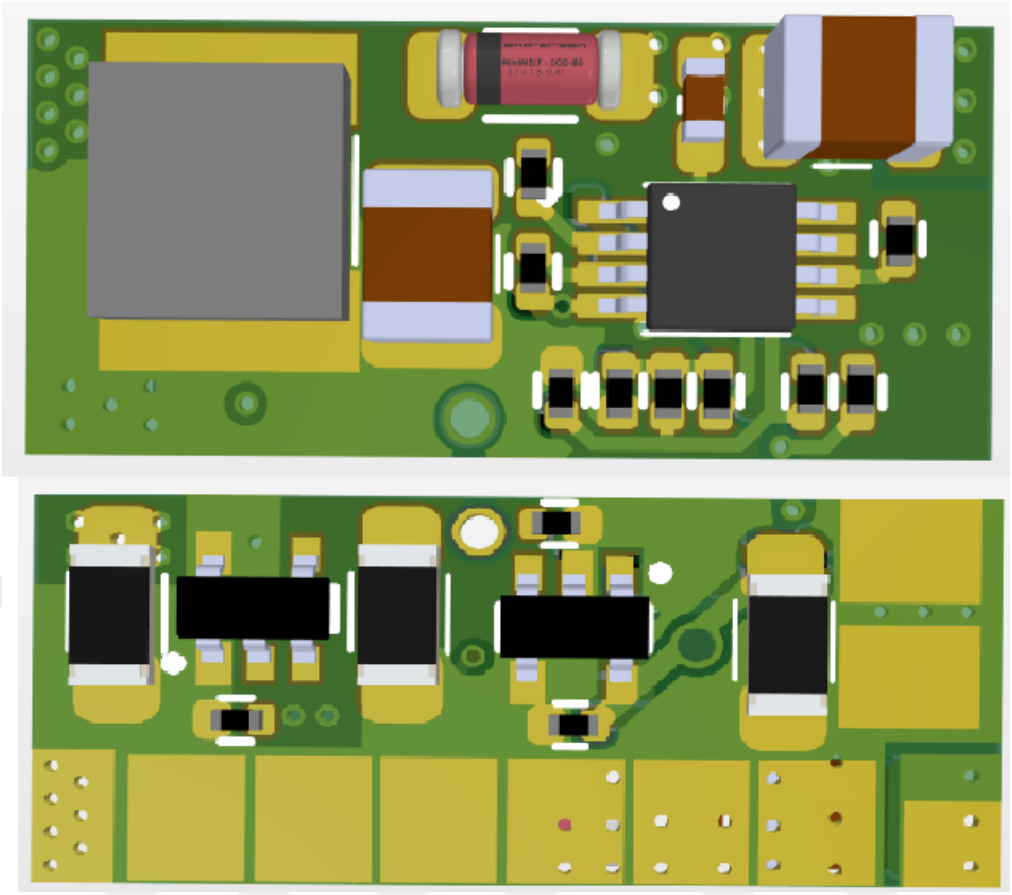

Figure 2.17 Regulator PCB 3D image

As shown in Figure 2.17 the regulator PCB is a different PCB from the main device. The aim of regulator PCB is a small sized DC-DC conver to supply MCU and gate drivers power. At the top of the regulator PCB has include a buck converter and at the output of the PCB has two stage cascade LDO regulator to provide 5V and 3.3V.

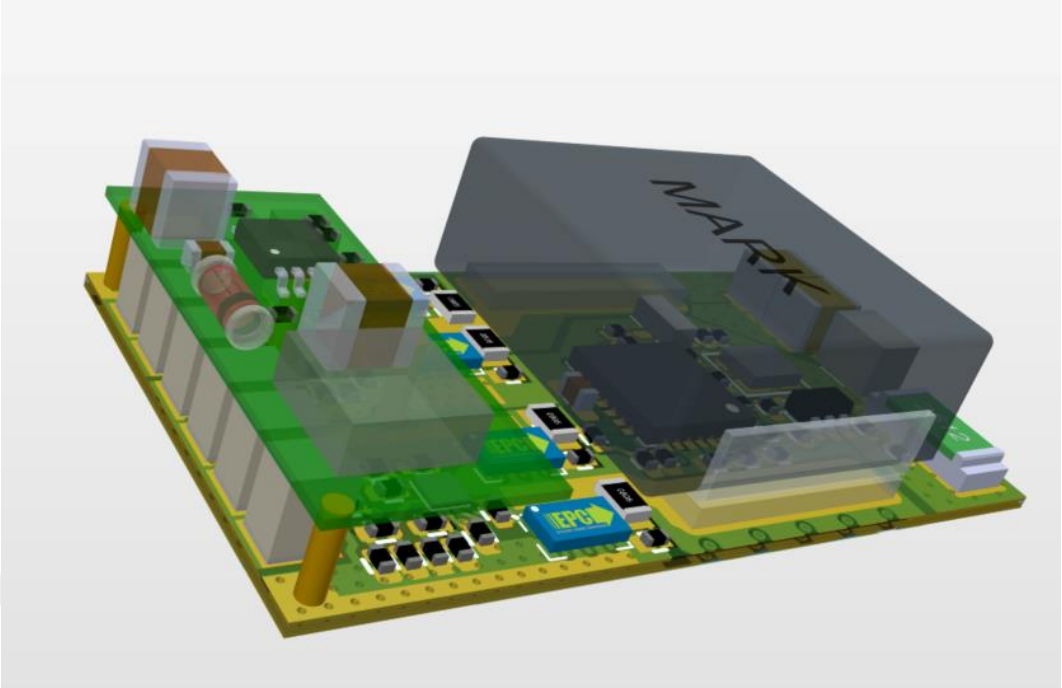

Figure 2.18 Stacked PCB 3D image

The regulator PCB and Main PCB are designed suitable to stach both of them together and solder. By stacking this PCB's the ceramic capacitors can be soldered vertically. One pad of the Ceramic capacitor is soldered main PCB and the other pad is soldered on Regulator PCB. When Ceramic capacitors soldered vertically we can create a strong structure with physical strenght. Also Input supply and ground connected to Regulator PCB with 0.5mm radius coppers. These coppers also increse stenght of the device.

2.6 Software Design

Embedded C coding for hyperloop systems plays a critical role in ensuring the efficient and reliable operation of these high-speed transportation networks. Hyperloop technology involves a complex integration of various subsystems, such as propulsion, levitation, navigation, and safety mechanisms, all of which require precise control and synchronization. Embedded C, a powerful and efficient programming language, is ideal for developing the real-time software that controls these subsystems. It allows engineers to write low-level code that directly interacts with the hardware, enabling fine-tuned performance and rapid response times crucial for the high speeds and safety standards of hyperloop systems. Furthermore, the robustness and portability of Embedded C make it suitable for use in the diverse and challenging environments encountered by hyperloop pods. Overall, Embedded C coding is fundamental to the development and success of hyperloop technology, providing the necessary tools to create a fast, safe, and efficient transportation system.

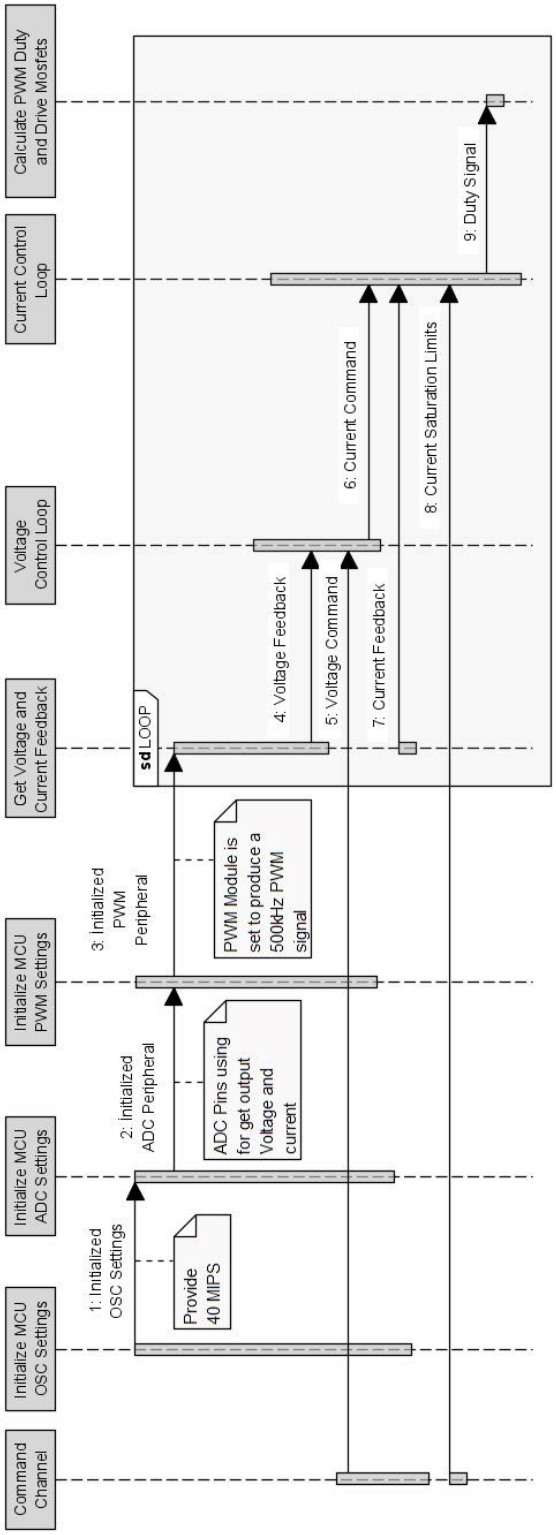

Figure 2.19 Software sequence diagram

Bi-directional non-inverting buck-boost converter sequence diagram illustrated in Figure 2.19. This figure shows The initialisation phase and feedback, control, duty relations.

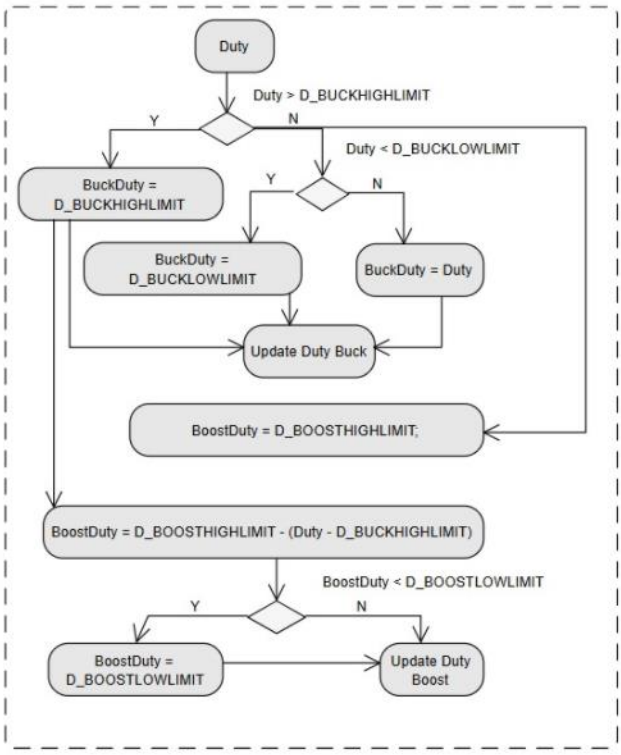

Figure 2.20 Buck and boost control algorithm

Control algorithm uses same duty calculated from Cascade PI blocks. When duty overflows buck high limit, it also means that the input voltage is lower than output voltage. The control algorithm start to decrese boost duty to provide higher output voltage until reach boost gain limit. The algorithm is shown in Figure 2.20

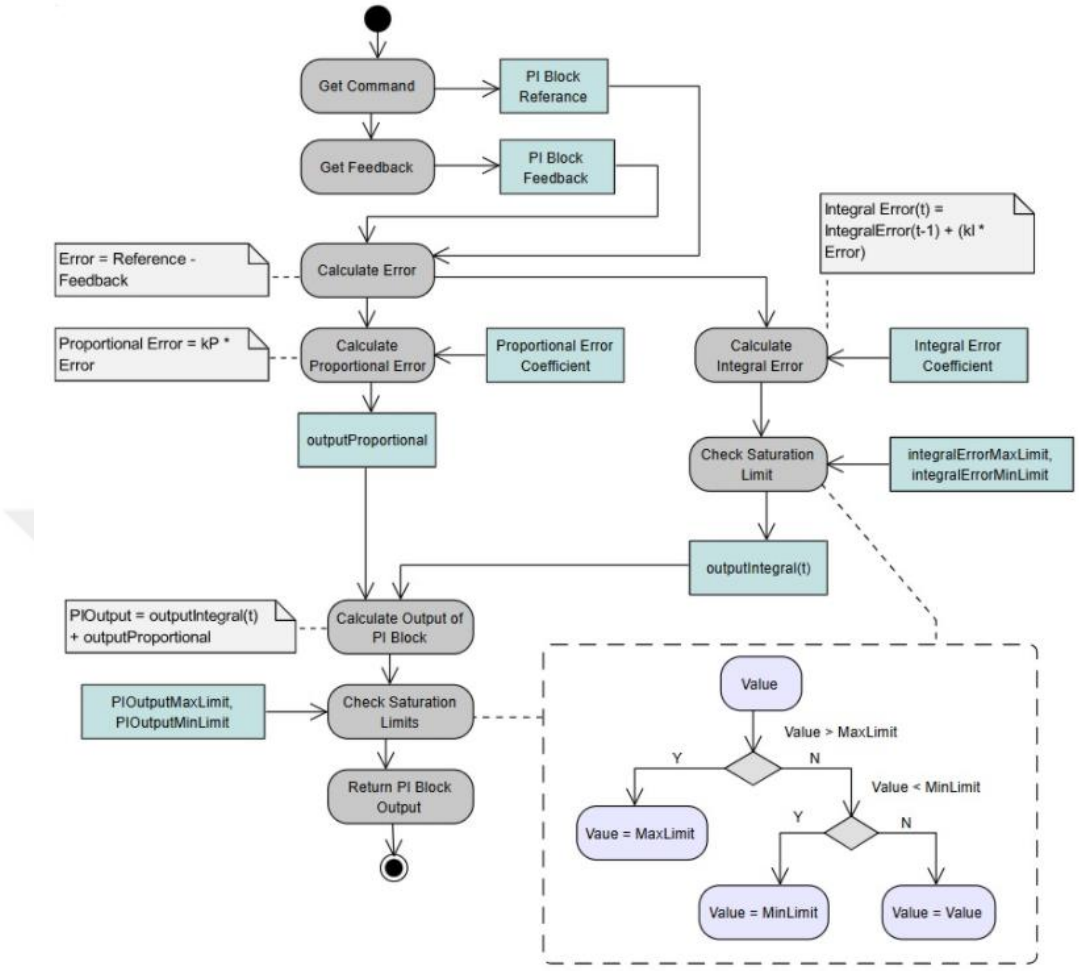

Figure 2.21 PI algorithm with output saturation

Bi-directional non-inverting buck-boost converter has an output voltage feedback and current feedback. Embedded software can regulate output voltage by using output voltage and current feedback and also the software can perform bidirectional working with only these two feedback. The software adopts two PI control block. Both block has own Integration and Output saturation limits to provide protection duty over flow and Integral overflow. Flow chart of the PI control algorithm is illustrated in Figure 2.21 .

2.7 Snubber Design

Snubber design is an essential aspect of electrical engineering, particularly in the context of protecting semiconductor devices and enhancing the performance of power electronic circuits. Snubbers are circuit elements, typically composed of resistors, capacitors, and sometimes inductors, that are used to suppress voltage spikes, dampen oscillations, and mitigate electromagnetic interference (EMI) generated during the switching events of power devices such as transistors and thyristors. Effective snubber design ensures the reduction of stress on these components, thereby prolonging their lifespan and improving overall circuit reliability. According to a study published in the IEEE Transactions on Power Electronics, carefully designed snubbers can significantly decrease the rate of voltage and current change (dV/dt and dI/dt), which in turn minimizes switching losses and thermal dissipation [47]. Key considerations in snubber design include the proper selection of component values to match the specific needs of the circuit, as well as ensuring that the snubber circuit does not adversely affect the system's efficiency or operation.

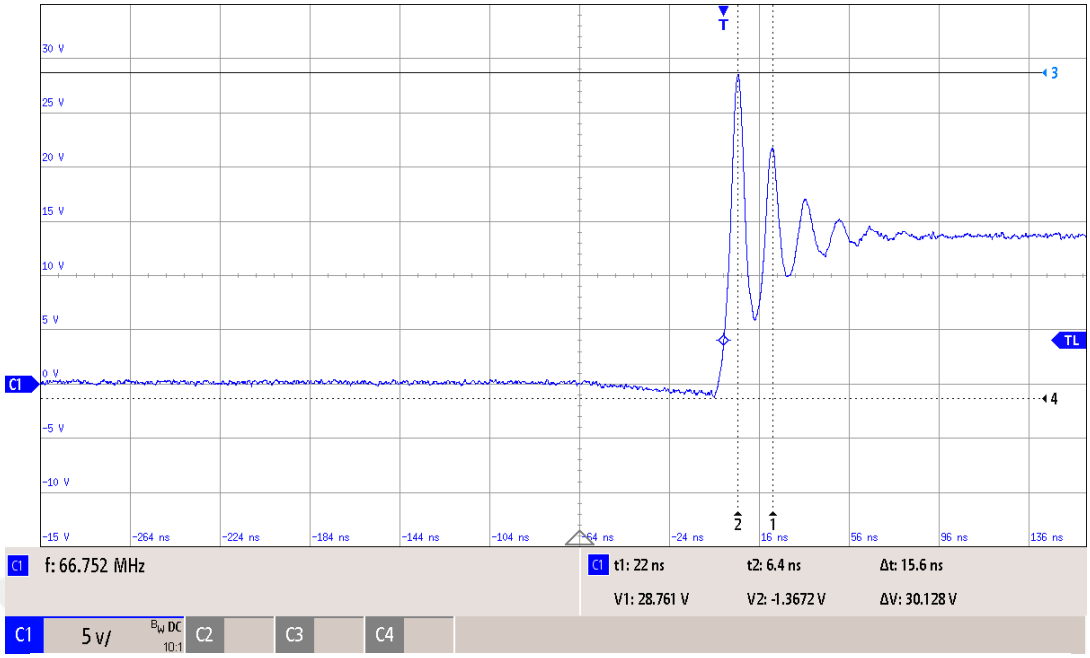

Figure 2.22 Drain-source measurements with 1Ω 100pF snubber components

In this design The snubber optimisation started with 13V input voltage %50 constant buck and boost duty and 1 Ω gate resistance 1 Ω Snubber resistance, 100pF snubber capacitance the device tested with this components and results is shown in Figure 2.22

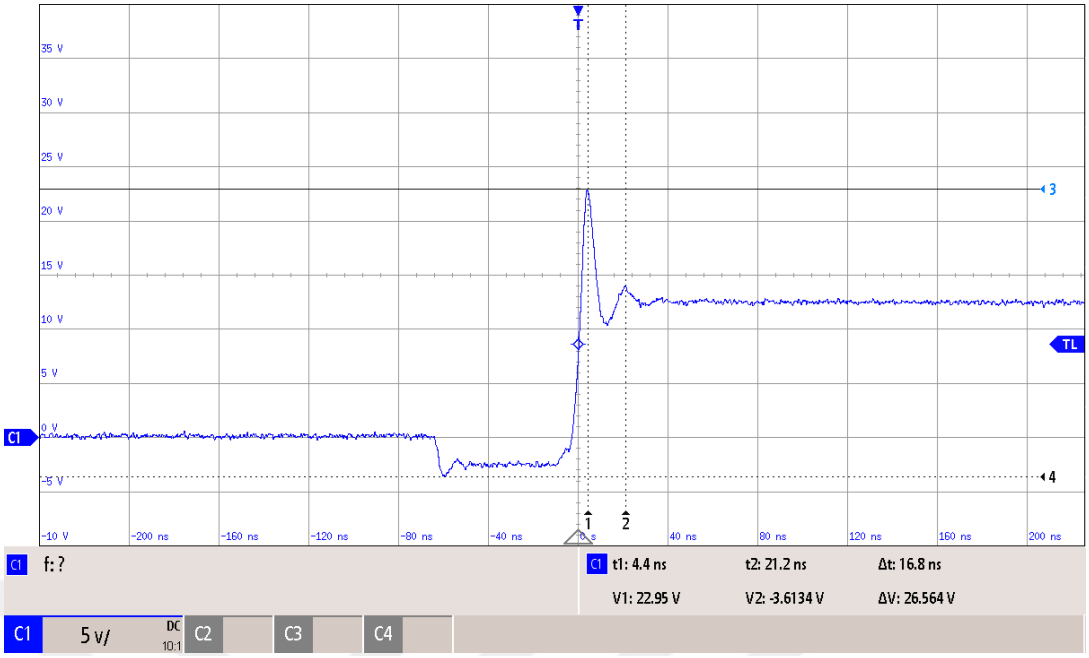

Figure 2.23 Drain-source measurements with 5Ω 2nF snubber components

After reaching results the snubber design is optimised to mimize ripple of the drain source voltage and also power dissipation of the snubber resistance considered. After couple of tests and simulations optimum gate resistance, snubber resistance and snubber capacitance calculated as 3.3 Ω gate resistance, 5 Ω snubber resistance and 2nf snubber capacitance. After applying this optimisations on hardware the Drain-Source voltage of GaN Fets measured, results is shown in Figure 2.23

CHAPTER 3

RESULTS & DISCUSSION

3.1 Simulation Results

Simulation circuit shown in Figure 2.9. the control block places underneath of the power components. PWM signals generated for high side switches, then the signal inverted for low side switches.

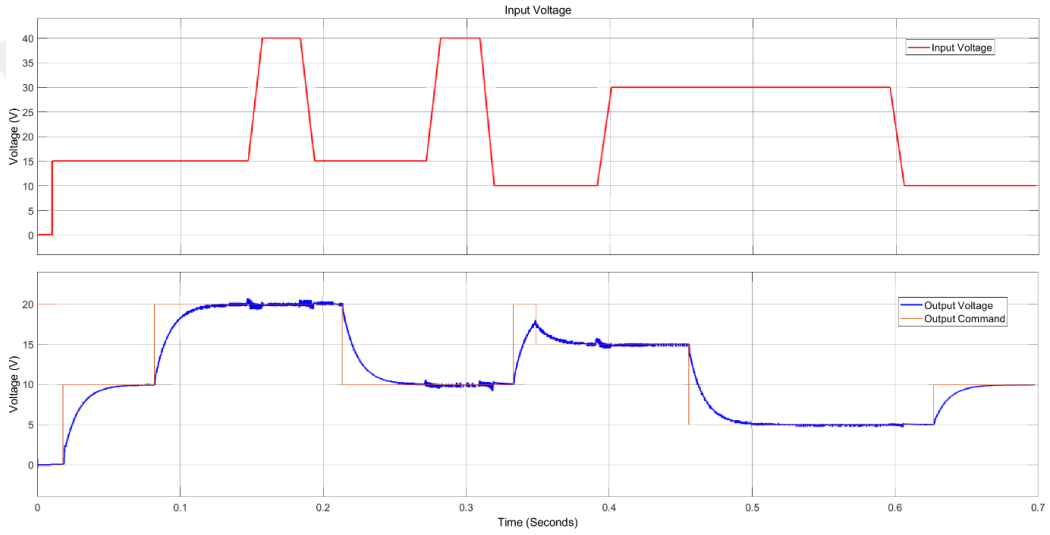

Figure 3.1 Dynamic response of proposed topology

The simulation results shown in Figure 3.1, represents the relation between, the change in input voltage and output voltage regulation. The applied input signal's rise time is shorter than 10 ms, it means the rate of change of the input voltage reaches 300 V/s the circuit can handle these rapid changes under %10 ripple at output. And, when output voltage reference is changed the actual output voltage follows the reference. The results show also, switching buck mode to boost mode or vice versa is occurred very smoothly and doesn't cause any ripple at the output.

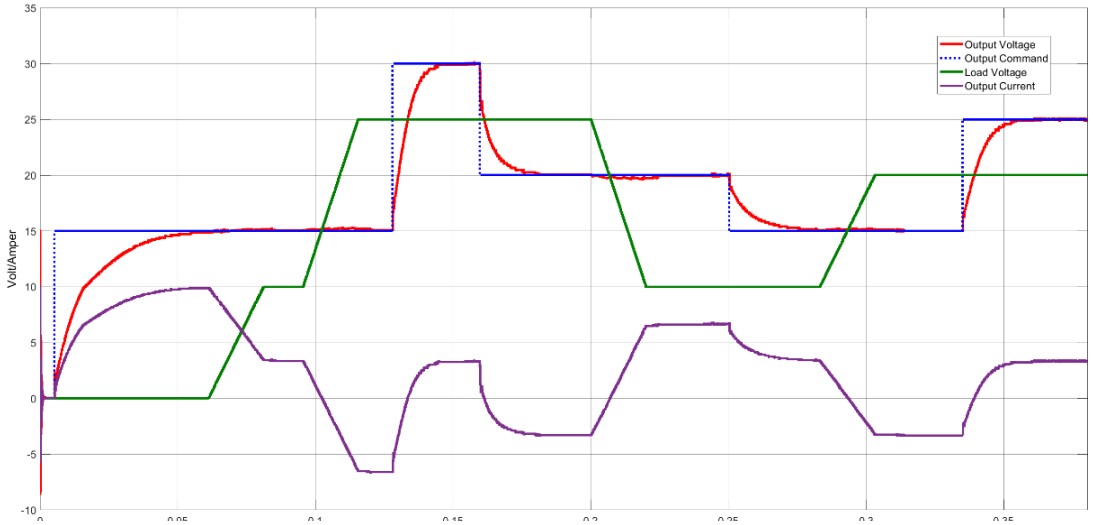

Figure 3.2 Dynamic response for bi-directional working

As shown in Figure 3. the direction of the output current defined from output voltage and load voltage, if load voltage bigger than output voltage, the current goes negative, that means current flows from load to input. But if output voltage is bigger than load voltage the output current goes positive that means the current flows from input to output. By this way bidirectional working is proved. The results show that bidirectional operation is achieved in both buck mode and boost mode, without being affected by the input voltage and without causing any ripple at the output. The load is modified to perform bidirectional working, and the simulation circuit is shown in Figure 2.8.

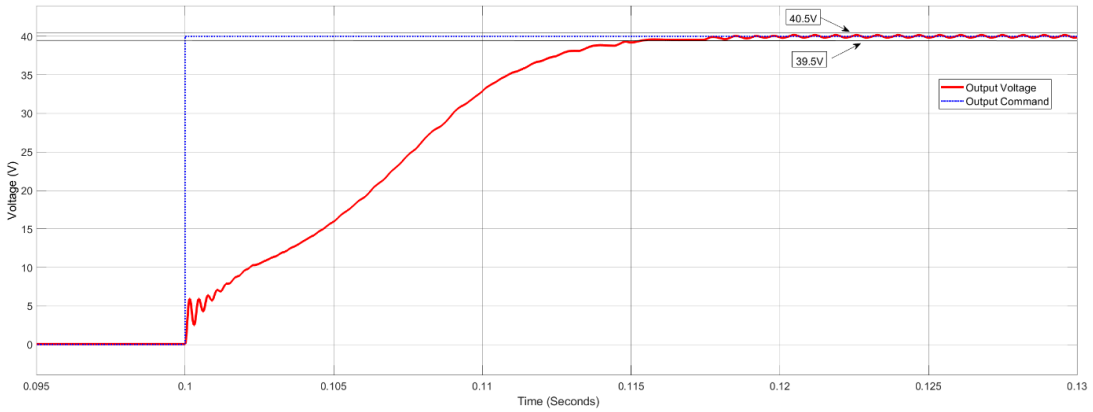

Figure 3.3 Output voltage ripple

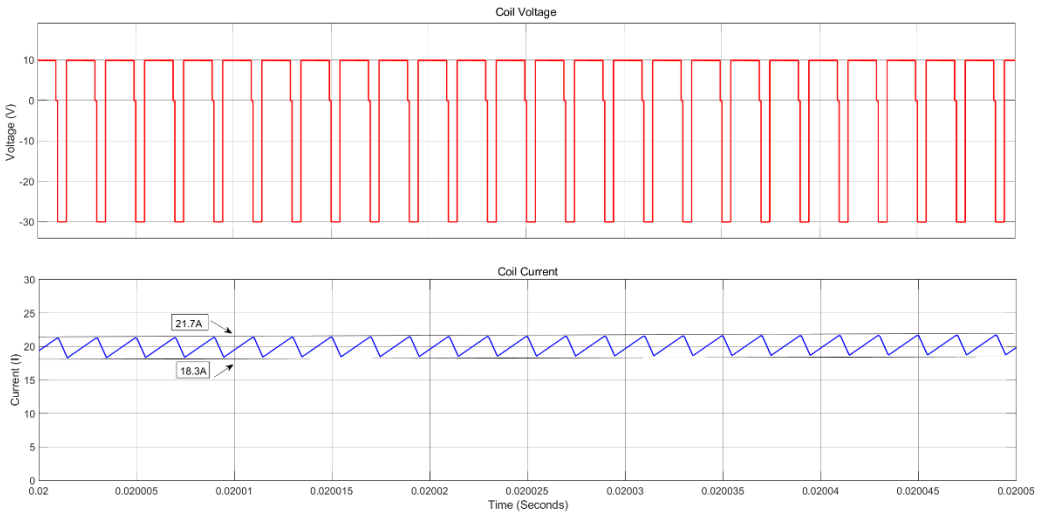

Figure 3.2 Coil voltage and current

Output voltage ripple shown in Figure 3. that shows the ripple voltage stays under 1V for 40V output it means %2.5 output ripple. The ripple can be reduced by adding extra output filter for higher accuracy applications

For practical applications the higher current ripples are main reason of electrical noises. In this research the simulation and theorical calculations shows that the ripple currents of the inductor stay under 4A. By this way the expectation for practical application EMI issues will be reduced.

The simulation results clearly show that, circuit can regulate output voltage in various range of input voltage and, the circuit can operate in various range of output voltage. And, for boost operation the voltage ripples are increased because of non-linearity of the system [48].

3.2 Experimental Studies

In this section, the results of the experiments obtained from the Non-Inverting Buck-Boost converter. The proposed circuit under test made by a "DSPIC33FJ32MC" MCU which runs control algorithm and creates switching signals. The MCU measures input voltage, output voltage and output current respectively. By using this feedback, it runs a PI control likely in our Simulink simulation. Same parameters are used, and controller loop time is same with Simulink settings. A H-bridge topology that includes four "EPC2060" (GaN-FET) and two "uP1966E" (GaN-FET gate driver) components. The components run at 500khz switching frequency. A "LM5007" buck converter designed to supply MCU and gate drivers. The circuit shown in Figure 3.3

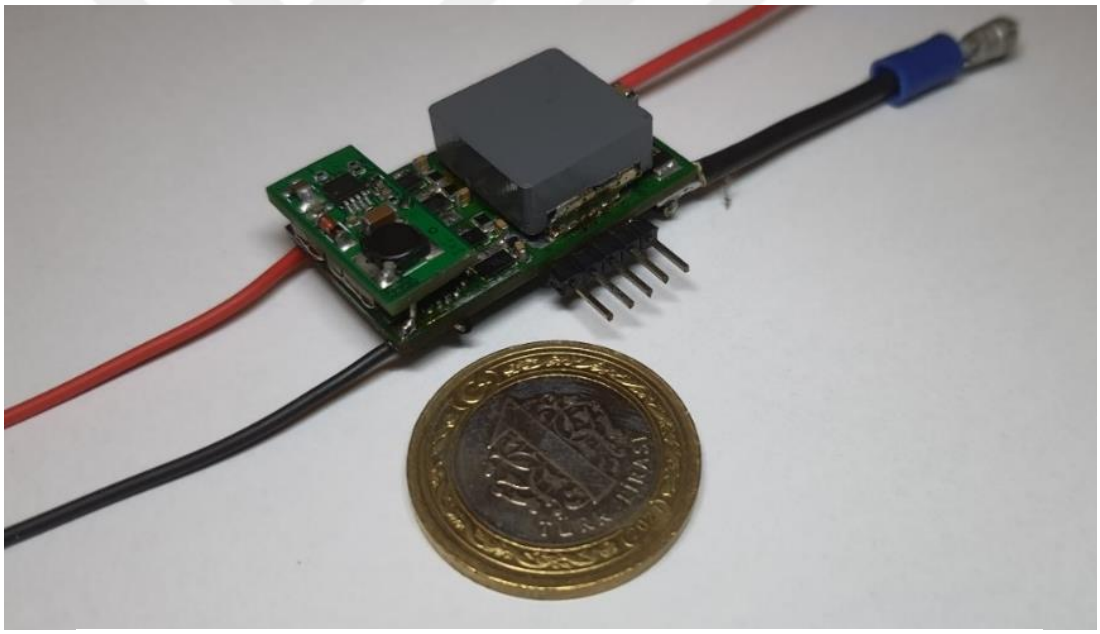

Figure 3.3 Bidirectional non-inverting buck-boost converter

The purposes of the test are:

Thermal Results: Non-Inverting Buck Boost converter tested under full load. The temperature is measured with thermal camera.

Efficiency: Non-Inverting Buck Boost converters input current and voltages measured between 10V to 40V range in every 5V. Output voltage and current measured for 12V, 15V, 24V and 30V fixed output reference voltage.

Response of controller: Effects of instant changes on input voltage and load to output voltage are observed.

Steady State Noise: Circuit tested for 30V input voltage, no load, 4A loaded and 9A loaded at 15V constant output voltage the steady state noise is observed with oscilloscope.

Start-up of Circuit: When first energized the Non-Inverting Buck Boost converter, response of the proposed circuit is observed.

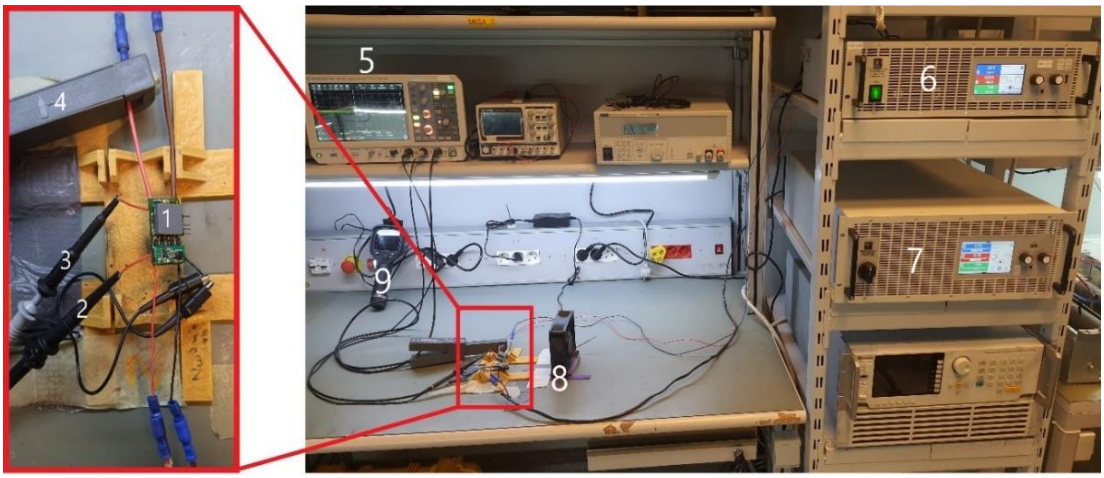

Figure 3.4 Test setup of bidirectional non-inverting buck-boost converter

The test setup shown in Figure 3.4 Test setup of bidirectional non-inverting buck-boost converter and the test equipments listed on Table 3.1.

Table 3.1 List of equipments for test

Number	Equipment
1	Non-Inverting Buck-Boost Converter (Equipment Under Test)
2	Oscilloscope Voltage Probe (CH2)
3	Oscilloscope Voltage Probe (CH1)
4	Oscilloscope Current Probe (CH3)
5	Oscilloscope
6	Electronic Load
7	Programmable Power Supply
8	Cooling Fan
9	Thermal Camera

For the Bidirectional Non-Inverting Buck-Boost Converter encompasses a comprehensive array of instruments and equipment tailored for precise evaluation. A programmable power supply, facilitating the precise adjustment of input voltages to simulate various operating conditions. An electronic load, enabling controlled loading of the converter to assess its performance under different output conditions. To manage thermal considerations, a cooling fan is integrated into the setup.

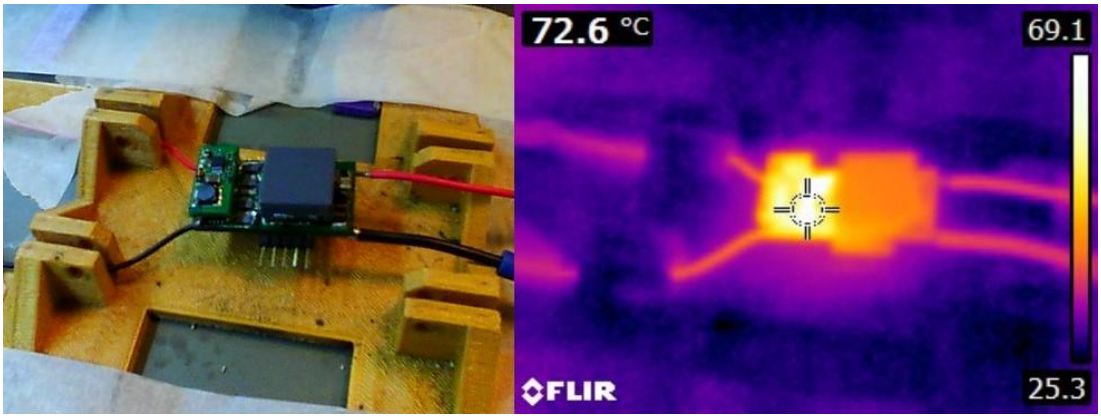

Figure 3.5 Full load thermal measurements

Additionally, a thermal camera provides thermal imaging to monitor temperature distributions across critical components. For electrical measurements, an oscilloscope equipped with two voltage probes is employed to accurately measure input and output voltages at the same time, while a current probe allows for the precise monitoring of input and output currents. Together, this comprehensive setup enables thorough testing and analysis of the Bidirectional Non-Inverting Buck-Boost Converter, facilitating the characterization of its electrical and thermal performance across a range of operating conditions.

Despite utilizing a fan for cooling instead of more advanced methods like liquid cooling or a cold plate and under the demanding conditions 30V input and 12V, 5A output representing the maximum power and least efficient operation region the thermal measurements of the Non-Inverting Buck Boost converter show promising results. Even with the heat generated by the GaN FETs the maximum temperature observed is a manageable 73°C. This suggests efficient heat dissipation, highlighting the effectiveness of the fan-based cooling system. The GaN FET’s transfers heat mostly with 2 oz(70um) thick copper planes which designed on PCB right under the Gan FET’s. By this way the GaN FET’s transfers heat in conduction method and distribute as wide area as possible on PCB. In summary, the thermal performance underscores the converter's robust design and its ability to maintain optimal operating conditions with a fan-based cooling solution.

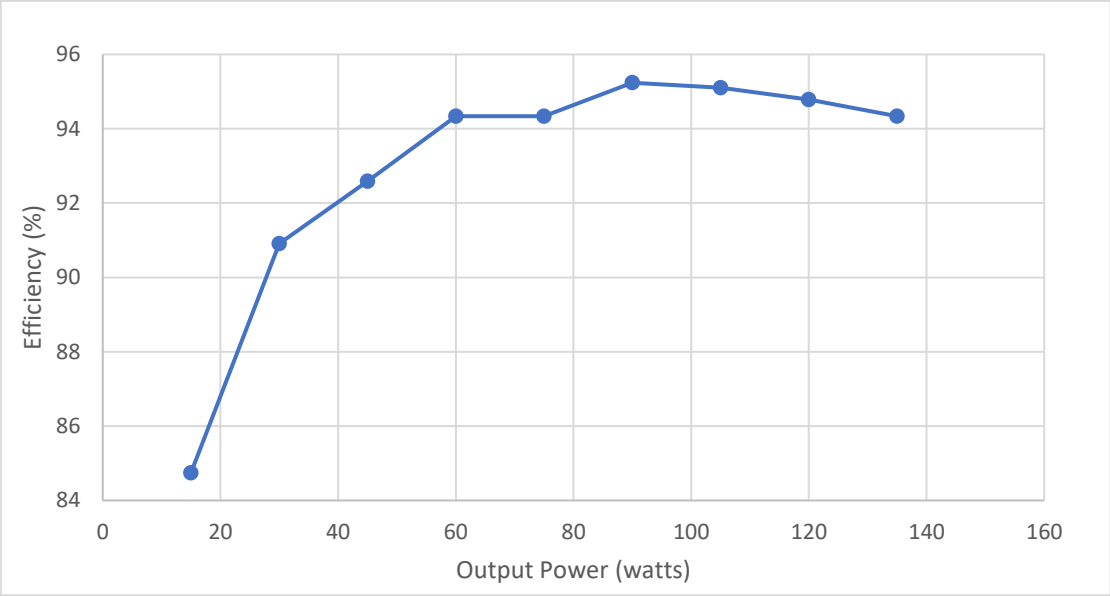

Figure 3.6 Efficiency vs output power

As shown in Figure 3.6, under the conditions of a 30V input and 15V output voltage, the Non-Inverting Buck Boost converter attained peak efficiency, reaching an impressive %95.2. This optimal efficiency was achieved when the input voltage was maintained at 30V, drawing 3.15A, corresponding to an input power of 94.5 watts, while simultaneously producing a 15V output at 6A, equivalent to 90 watts of output power. Notably, throughout the power range spanning from 60 watts to 135 watts, and across virtually all operational scenarios, the converter consistently demonstrated efficiencies exceeding %94.

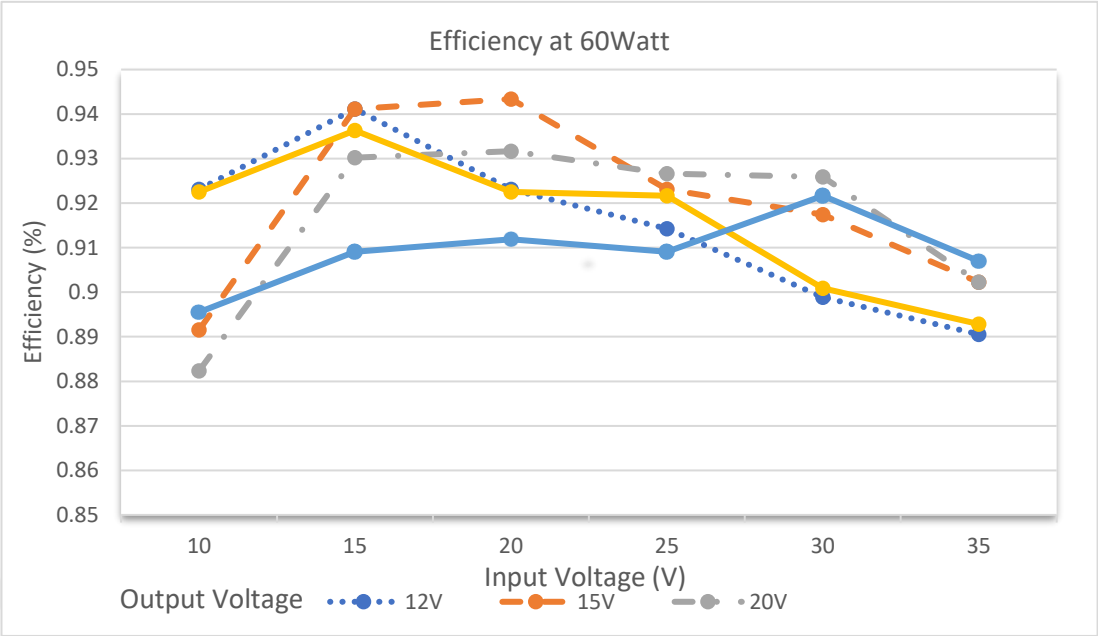

Figure 3.7 Efficiency with respect to input and output voltages at 60 watt

The Non-Inverting Buck Boost converter tested to analyze the impact of varying input and output voltages on efficiency. A constant 12V, 5A output, tests performed across a range of input voltages, from 10V to 35V. Input and output voltages, along with corresponding currents, were measured using an oscilloscope, with the results depicted by dashed blue lines in Figure 3.7. The experimentation was then extended to encompass different output configurations: 15V at 4A, 20V at 3A, 25V at 2.4A, and 30V at 2A. Each set of results was recorded and illustrated in Figure 3.7. Intriguingly, the data analysis revealed that the peak efficiency of %94 was achieved under the conditions of a 15V output at 4A with a 20V input. This finding underscores the critical relationship between input and output voltages in determining the converter's efficiency and highlights the significance of optimizing these parameters for enhanced performance.

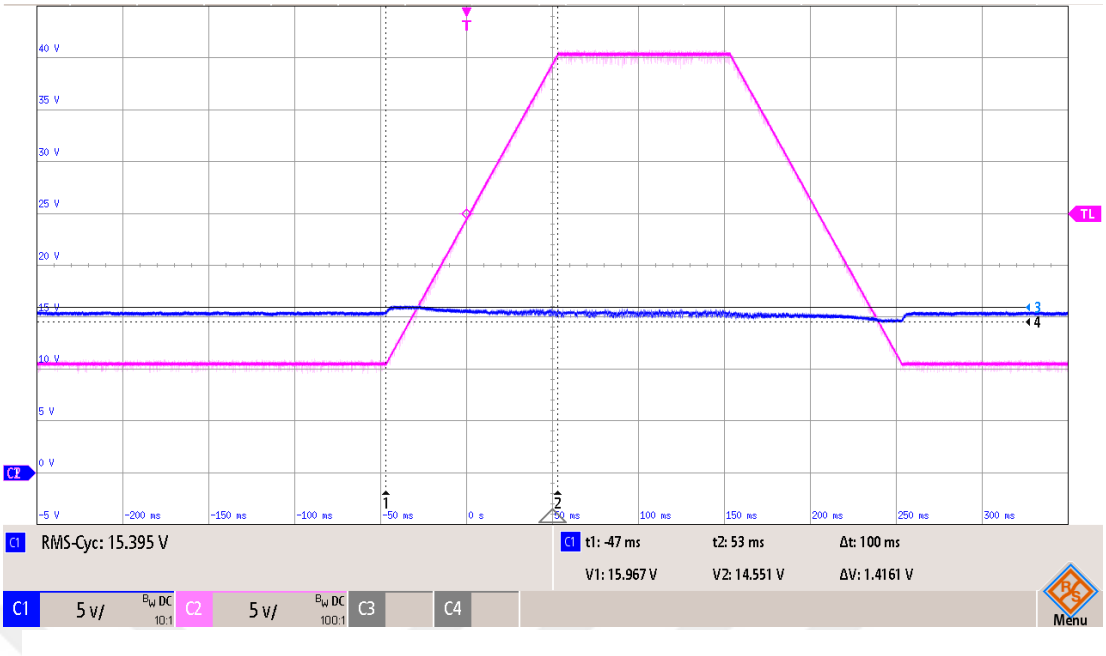

Figure 3.8 Effect of input voltage variation

Input voltage is supplied from a programmable voltage supply the voltage supply programmed for trapezoidal shaped voltage. The input voltage is increased from 10V to 40V in 100ms. Then the voltage decreased from 40V to 10V. The effect of the input voltage to output voltage is represented in Figure 3.8 Effect of input voltage variation.

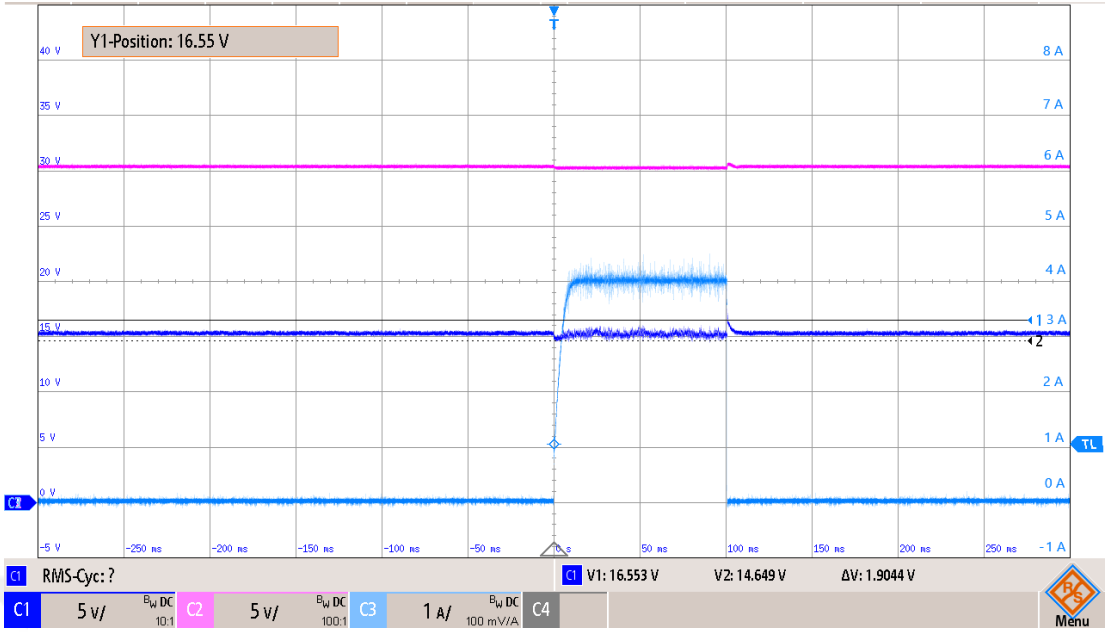

Figure 3.9 Load Variation from no load to half load, and vice versa

Load variation is real challenge for DC-DC converters. In Figure 3.9 Load Variation from no load to half load, and vice versa you can see the load current increased 0A to 4A under 10ms. The change in output current is reflected in the output voltage. While load current is instantly increasing, we can see output voltage is decreased as expected. The decrease of the output voltage is measured 0.351V (15V-14.649). While output current is decreased instantly from 4A to 0A under 1ms. The increase of the output voltage is measured 1.553V (16.553V-15V).

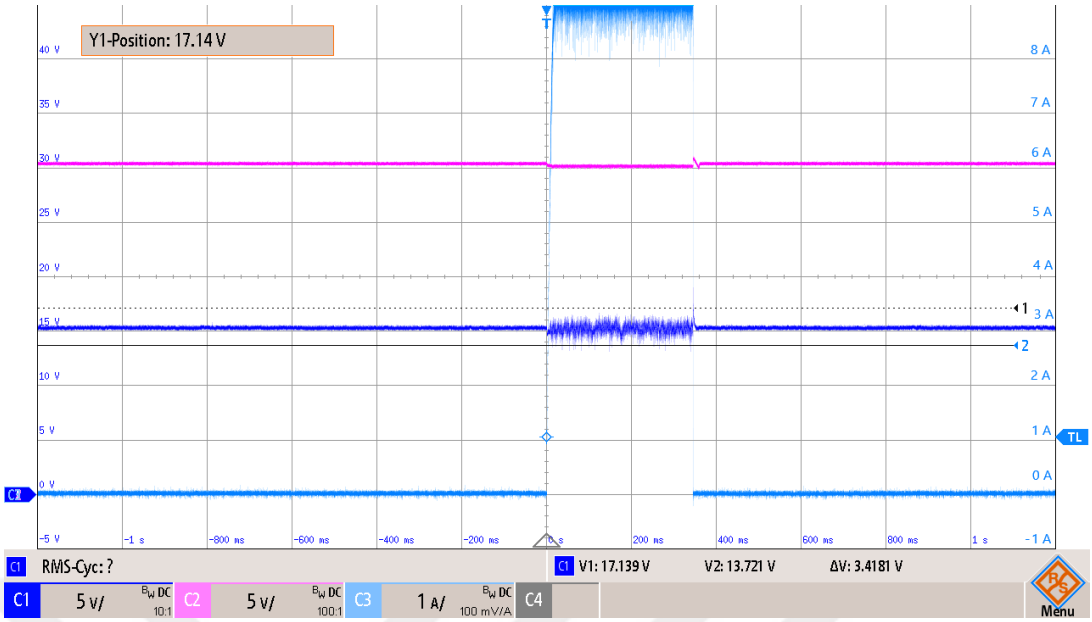

Figure 3.10 Load variation from no load to full load, and vice versa

In Figure 3.10 Load variation from no load to full load, and vice versa. you can see the load current increased 0A to 9A under 10ms.The decrease of the output voltage is measured 1.3V (15V-13.7V). While output current is decreased instantly from 9A to 0A under 1ms. The increase of the output voltage is measured 2.1V (17.1V-15V).

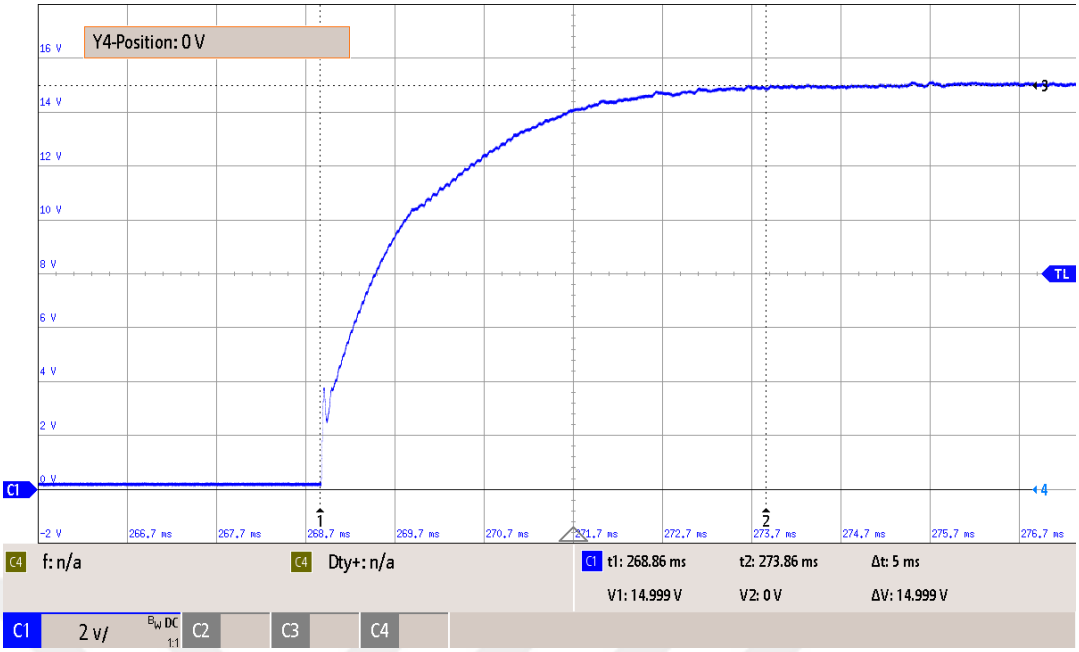

Figure 3.11 Step response of non-inverting buck-boost converter

The start-up time of the Non-Inverting Buck Boost converter defined as the time of the circuit's output voltage reaches the reference voltage. In Figure 3.11 Step response of non-inverting buck-boost converter we can see the start-up of the circuit which reference voltage is 15V at 10V input voltage. The circuit is turns on at 10 V input voltage and 1ms is initializing time of software after that time the output voltage starts to increase. The increase time is measured 10ms for this configuration. Depending on application the startup time can be programmable on software.

CHAPTER 4

CONCLUSION

The designed and tested circuit is measured 20x37x9 mm (0.4 in^3) and is capable of delivering an output power of 150W, resulting in a power density of 375 watts per cubic inch. Experimental results have demonstrated not only the variation of input and output voltage range but also the high efficiency and power density of the circuit. The high-frequency output noise of the circuit was observed during testing. By incorporating a small output filter, the output noise can be significantly reduced. Furthermore, utilizing advanced heat dissipation techniques can further enhance both efficiency and power density. Detailed comparisons between simulation and experimental results are confirmed the accuracy of the proposed circuit's performance metrics. Specifically, the output noise levels, the relationship between input and output, and overall efficiency are consistent with theoretical application. This alignment between simulations and experimental outcomes underscores the reliability and effectiveness of the circuit design and operational parameters.

Despite its advantages, this circuit suffers from the drawback of hard switching and a non-isolated structure. In future studies, with maintaining power density while addressing these issues, Full-Bridge LLC or Phase-Shifted LLC topologies could be explored. These topologies would allow for a transition to an isolated structure while also improving efficiency through soft switching. Additionally, the circuit's high efficiency, wide input voltage range, and compact dimensions make it suitable for use in cascade topologies, potentially expanding its range of applications.

REFERENCES

[1] Colino, S.L. and Beach, R.A., "*Fundamentals of Gallium Nitride Power Transistors*", Application Note, 2009

[2] Shoihet, A. & Slonim, M.A., "*Analysis of transient processes of buck-boost converter: Theoretical analysis, physical experiments, modeling and simulati*on", Annual Conference on IEEE Industrial Electronics Society, *38,* 5365-5369, 2012.

[3] Midya, P., Haddad, K., & Miller, M., "*Buck or boost tracking power converter*", IEEE Power Electronics Letters, *2,* 131-134, 2004.

[4] Tsai, C.H. & Tsai, Y.S., "*A Stable Mode-Transition Technique for a Digitally Controlled Non-Inverting Buck-Boost DC-DC Converter*", IEEE Transactions on Industrial Electronics, *62*, 475-483, 2014.

[5] Agamy, M.S., Chi, S. & Elasser, A., M. Harfman, T., Jiang, Y., Mueller, F., Tao F., "*A High-Power-Density DC–DC Converter for Distributed PV Architectures*", IEEE Journal of Photovoltaics, *3*, 791-798, 2013.

[6] Prodic, A., & Maksimovic, D., "*Design of a digital PID regulator based on look-up tables for control of high-frequency DC-DC converters*", IEEE Workshop on Computers in Power Electronics, 18-22, 2002.

[7] Luo., F. and Ma, D., "*Design of digital tri-mode adaptive output buck-boost power converter for power-efficient integrated systems*", IEEE Transactions on Industrial Electronics, *57*, 2151-2160, 2010.

[8] Zhang, F., Du L. and Quian, Z., "*A New Design Method for High-Power High-Efficiency Switched-Capacitor DC–DC Converters*" IEEE Transactions on Power Electronics, *23*, 832-840, 2008.

[9] Wai, R.J. and Shih, L.C., "*Design of voltage tracking control for DC-DC boost converter via total sliding-mode technique*", IEEE Transactions on Industrial Electronics, *58*, 2502-2511, 2011.

[10] Shin, J. W., Ishigaki, M., Dede, E. M., Lee, J. S., "*MagCap DC–DC Converter Utilizing GaN Devices: Design Consideration and Quasi-Resonant Operation*", IEEE Transactions on Power Electronics, *34*, 2441-2453, 2018.

[11] Efficient Power Conversion Corporation. (n.d.) Retrieved from https://epc-co.com/epc/gallium-nitride/why-gan

[12] Sahay, S., Kumar, M. J., "*Introduction to Field-Effect Transistors*", Wiley-IEEE Press, ISBN:9781119523543, 2019.

[13] "*International Roadmap for Devices and Systems Executive Summary*", IEEE, 2023, ISBN:979-8-3503-2458-7, 2023

[14] Wolfspeed and the Biophysical Economics Institute Announce Pioneering Study That Demonstrates the Superiority of Silicon Carbide for Energy Efficiency. (n.d.). Retrieved from https://www.wolfspeed.com/company/news-events/news/wolfspeed-and-the-biophysical-economics-institute-announce-pioneering-study-that-demonstrates-the-superiority-of-silicon-carbide-for-energy-efficiency/

[15] Despite the current global economic challenges, the growth trajectory of SiC for power electronics remains intact (n.d.). Retrieved from https://www.yolegroup.com/press-release/yg-press-news-despite-the-current-global-economic-challenges-the-growth-trajectory-of-silicon-carbide-sic-for-power-electronics-remains-intact/

[16] Khan, J.M., Khan, A.A., Jamil, M., "*A Novel Non-Isolated Bidirectional DC-DC Converter with Improved Current Ripples for Low-Voltage On-Board Charging*", Energies, *17*, 14, 2024.

[17] Xu, X., Qihang, Z., Ma, T., Mai, S., "*A High Efficiency, Low EMI Non-inverting Buck Boost Converter in Wireless Power and Data Transfer System for Brain Computer Interface*", Brain Computer Interface: Hardware & Circuit Design, *99*, 1-1, 2018.

[18] Mumtaz, F., Meraj, S.T., Singh, B.S.M, Kannan, R., "*Review on non-isolated DC-DC converters and their control techniques for renewable energy applications*", Ain Shams Engineering Journal, 12, 3-4, 2021.

[19] Dileep, G., Singh S.N., "*Selection of non-isolated DC-DC converters for solar photovoltaic system.*", Renewable and Sustainable Energy Reviews, 76, 1230-1247, 2016.

[20] Hossain M.Z., Rahim N.A., Selvaraj, J., "*Recent progress and development on power DC-DC converter topology, control, design and applications: a review*", Renewable and Sustainable Energy Reviews, *81*, 1, 205–230, 2017.

[21] Moradpour, R., Ardi, H., Tavakoli A., "*Design and implementation of a new SEPIC based high step-up DC/DC converter for renewable energy applications.*", IEEE Transactions on Industrial Electronics, *65*, 2, 1290–1297, 2017.

[22] Lopez-Santos, O., Cabeza-Cabeza, A.J., Garcia, G., Martinez-Salamero L. "*Sliding mode control of the isolated bridgeless SEPIC high power factor rectifier interfacing an AC source with a LVDC distribution bus.*", Energies, *12*, 18, 2019.

[23] Sivakumar, S., Sathik, M.J., Manoj, P.S., Sundararajan, G., "*An assessment on performance of DC-DC converters for renewable energy applications.*", Renewable and Sustainable Energy Reviews, *58*, 1475–1485 2016;

[24] Siddharthan, N., Balasubramanian, B., "*Performance evaluation of SEPIC, Luo and ZETA converter.*", International Journal of Power Electronics Driver Systems, *10*, 1, 374-380, 2019.

[25] Keerthana, R., Chintu, NJ., "*Performance analysis of zeta converter in wind power application.",* Asian Journal of Applied Science and Technology *1*, 3,199–203, 2017.

[26] De Morais, J.C.D.S., De Morais, J.L.D.S., Gules, R., "*Photovoltaic AC module based on a ĆUK converter with a switched-inductor structure.*", IEEE Transactions on Industrial Electronics, *66*, 5, 3881–3890, 2019.

[27] Kummara, V.G.R., Kamran, Z., Anand, M., Krishna, T. N. V., Kim, D.H, Kim, H.G.C., Kim, H.J., "*Comprehensive review of DC–DC converter topologies and modulation strategies with recent advances in solar photovoltaic systems*", Advances in Power Electronics Technologies for Renewable Energy Systems, *9*, 1, 19, 2020.

[28] Reshma Gopi, R., Sreejith, S., "*Converter topologies in photovoltaic applications – A review.*", Renewable and Sustainable Energy Reviews, *94*, 1-14, 2018.

[29] Chen, F.Z., Jou, H.L., Wu, J.C., Hung, H.C., Luo, J.Y., "*An Online Maximum Efficiency Point Tracking Technique for Bidirectional Noninverting Buck–Boost Converter Over Wide Power Range*", IEEE Transactions on Power Electronics, *39*, 7, 7995-8006, 2024.

[30] Xiao, A. L., Ruan, B.X., "*The Bidirectional Four-Switch Buck-Boost Converter with PWM Plus Phase-Shift Control.*", International Power Electronics and Motion Control Conference, *10*, 2849-2853, 2024.

[31] Hernandez-Nochebuena, M.A., Araujo-Vargas, I., Velazquez-Elizondo, P.E., Cano-Pulido, K., Cervantes, I., Sosa-Savedra, J.C., "*High Power Density, Buck-Boost Converter with Dual Interleaved Four-Phase Coupling*", Transactions on Transportation Electrification, *10*, 1-1, 2024.

[32] Surya, P.P., Irawan, D., Zuhri, M., "*Review and comparison of DC-DC converters for maximum power point tracking system in standalone photovoltaic (PV) module*", International Conference on Advanced Mechatronics, Intelligent Manufacture, and Industrial Automation, 242–247, 2017.

[33] Marodkar, M., Adhau, S., Sabley, M., Adhau, P., "*Design and simulation of DC-DC converters for Photovoltaic system based on MATLAB*", International Conference on Industrial Instrumentation and Control, 1478–1483, 2015.

[34] Gangavarapu, S., Rathore, A.K. "*A three-phase single-sensor-based ĆUK-derived PFCconverter with reduced number of components for more*

electric aircraft.", Transactions on Transportation Electrification, *6*, 4, 1767–1779, 2020.

[35] Luo, J., "*Novel ĆUK-based bridgeless rectifier of wireless power transfer system with wide power modulation range and low current ripple*" IEEE Transactions on Industrial Electronics, *69*, 3, 2533–2544, (2022).

[36] Yang, J.W., Do, H.L., "*Bridgeless SEPIC converter with a ripple-free input current*", IEEE Transactions on Power Electronics, *28*, 7, 3388–3394, 2013.

[37] Moradpour, R., Ardi, H., Tavakoli, A., "*Design and implementation of a new SEPIC based high step-up DC/DC converter for renewable energy applications*", IEEE Transactions on Industrial Electronics, *65*, 2, 1290–1297, 2018.

[38] Ardi, H., Ajami, A., "*Study on a high voltage gain SEPIC-based DC–DC converter with continuous input current for sustainable energy applications*", IEEE Transactions on Power Electronics, *33*, 12, 10403–10409, 2018.

[39] Zhu, B., Liu, G., Zhang, Y., Huang, Y., Hu, S., "*Single-switch high step-up zeta converter based on coat circuit*", IEEE Access, *9*, 5166–5176, 2021.

[40] D. Murthy-Bellur, M.K. Kazimierczuk, "*Isolated two-transistor zeta converter with reduced transistor voltage stress*", IEEE Transactions on Circuits and Systems II: Express Briefs, *58*, 1, 41–45, 2011.

[41] Fundamentals of PID Control (n.d.). Retrieved from. https://www.isa.org/intech-home/2023/june-2023/features/fundamentals-pid-control

[42] Cuk, S., Smedley, K.M., "*One-cycle control of switching converters",* IEEE Transactions on Power Electronics, *10*, 625-633, 1995.

[43] Habib, S., Khan, M.M., Abbas, F., Ali, A., Faiz, M.T., Ehsan, F., Tang, H., "Contemporary trends in power electronics converters for charging solutions of electric vehicles". CSEE Journal of Power and Energy Systems, *6*, 2020.

[44] Edwards, C., Spurgeon S., "*Sliding Mode Control: Theory and Applications*.", CRC Press, *1*, 191-212, 1998.

[45] Erbatur, K., Kaynak, M.O., Sabanovic, A., "*A study on robustness property of sliding-mode controllers: a novel design and experimental investigations*.", IEEE Transactions on Industrial Electronics, *46*, 1012-1018, 1999.

[46] Wu, T.L., Buesink, F., Canavero, F., "*Overview of Signal Integrity and EMC Design Technologies on PCB: Fundamentals and Latest Progress.*" IEEE Transactions on Electromagnetic Compatibility, *55*, 624-638, 2013.

[47] Paul, R. and Maksimovic, D., "*Analysis of PWM nonlinearity in non-inverting buck-boost power converter*s", IEEE Power Electronics Specialists Conference, 3741-3747, 2008.

[48] Wu, Y., Yi, Q., Wu, Y., Yang, F., Zhang, Z., Wen, J., "*Research on Snubber Circuits for Power Electronic Switch in DC Current Breaking.*", IEEE Conference on Industrial Electronics and Applications, *14*, 2019.